№1, 2021

ISSN 2706-977X

MATERIAL AND MECHANICAL ENGINEERING TECHNOLOGY

Content

DOI 10.52209/2706-977X_2021_1_3 **IRSTI 55.03.14** **UDC 621.878**

Study and calculation of earth-moving machines for the construction by "wall in the ground" method

Kadyrov A.S. , Zhunusbekova Zh.Zh.*, Ganyukov A.A.
Karaganda Technical University, Karaganda, Kazakhstan
*corresponding author

Abstract: The authors developed and investigated a mathematical model of the movement of the excavating parts of drilling machines used in construction and mining. The block method of setting resistance to movement of excavating parts is used. Dependencies on loading, external forces and drilling speed are obtained which determine machine efficiency. The specific energy intensity of the process was optimized. The article regards rotary drilling machines.

Keywords: excavating part, cutting resistance, transportation resistance, clay solution, supply force, torque moment, bore bit, specific energy intensity.

1. Introduction

The main idea of the study is the possibility of obtaining the laws of motion of drilling machines by means of crossing loads in two sets: the functioning environment and the constructions of the transporter. At the same time, it is not necessary to model the operation of each machine separately.

The purpose of the study is to obtain dependencies describing the speed of supply (productivity) of the excavating part in various working conditions, and scientific novelty is determined by obtaining these dependencies.

A large number of drilling machines are used in construction and mining: the "wall in the ground" method; bored piles; anchoring of slopes; blast hole drilling. The acquisition of new machines is very expensive, the modernization of their excavating parts is relevant.

To do this, we need to obtain dependencies on which we can base the calculation method.

Ground destruction (cutting) by the excavating part of the drilling machine can occur in a dry bottom or under a layer of clay mortar (keeping the walls of the well from breaking), transportation of the destroyed ground is carried out by an auger, elevator, shovel, screw, airlift, ground pump (Figure 1).

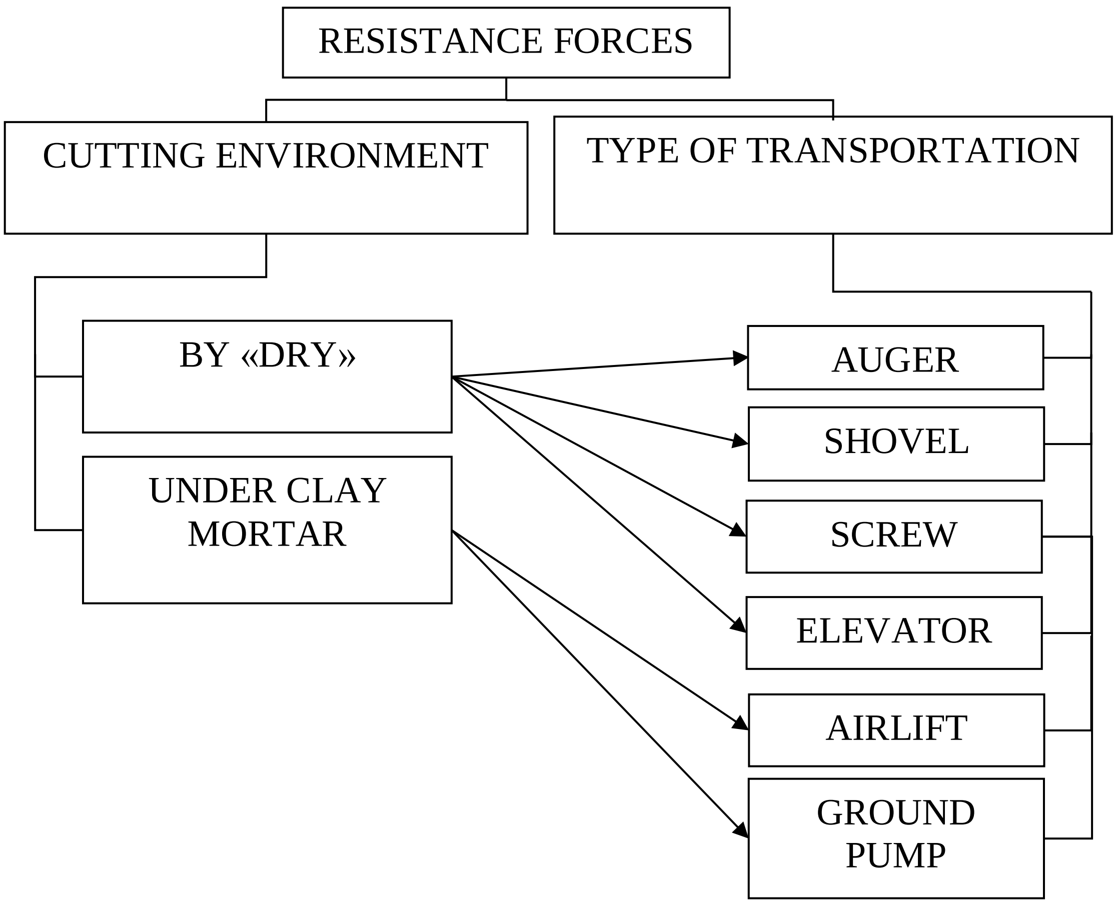

Fig. 1. - Classification of resistance forces of excavating parts

The hypothetical model of the excavating pert is generally influenced by the following set of forces: gravity force mg, supply force Q, torque moment M_t, cutting resistance M_{res}, supply resistance Q_c, motion resistance and transporter speed P_{tr}, motion resistance in the clay mortar Q_{cl} and M_{cl}, expulsive force P_{exp}, friction force of the excavatig part rod against the clay mortar P_{fr} [1].

The force scheme is shown in Figure 2.

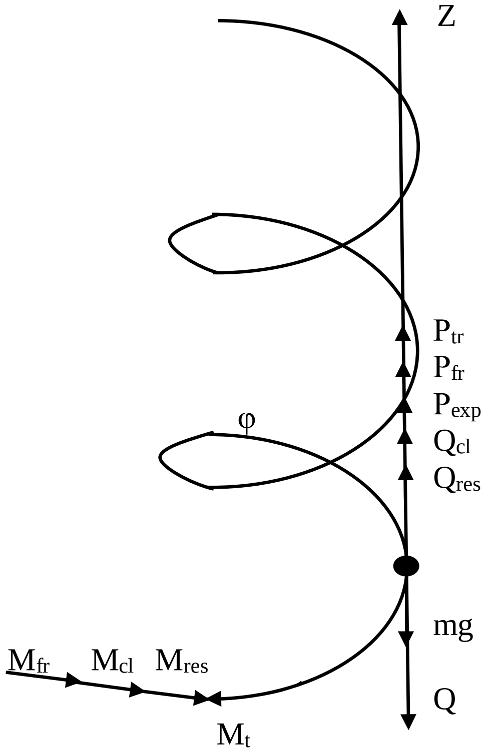

Fig.2. - General scheme of forces acting on the excavating part of the drilling machine

Resistance forces are determined [2] through specific forces of supply A and rotation B of bore bit; coefficient k_p, which takes into account the hydrodynamic component of motion resistance of the excavating part in the clay mortar; coefficient α_z of correction value of specific forces A and B in liquid environment of drilling. All these parameters are determined theoretically and confirmed experimentally in the work of the professor Kadyrov A.S. [3, 4].

The general system of equations in the directions of motion Z and φ has the form:

$$\begin{cases} m\ddot{z} = Q - Q_{res} - Q_{cl} - P_{exp} - P_{fr} - P_{tr} + mg \\ J\ddot{\phi} = M_t - M_{res} - M_{cl} - M_{fr} \end{cases}, \quad (1)$$

or disclosing the force expression taking into account the above factors:

$$\begin{cases} m\ddot{z} = Q - A\alpha_z Z - k_{в} Z - k_\delta Z - P_{mp} + mg \\ J\ddot{\varphi} = M_t - B\alpha_z ZR - k_p\omega^2 - M_{fr} \end{cases}, \quad (2)$$

where h - cutting depth per rotation;

k_b and k_δ - coefficients, respectively, which determine the expulsive friction force per one meter of the length of the excavating part;

m - weight of the excavating part;

$\ddot{z}$- linear acceleration of the excavating part motion;

J - moment of inertial forces from the rotating excavating part;

$\ddot{\varphi}$ - angular acceleration of the excavating part motion.

The force Q_{cl} of the vertical component of the rotation of the bore bit in the clay mortar is not taken into account due to its smallness.

The resistance force to transporting may depend on the depth of drilling Z or be constant:
for airlift and ground pump: $P_{tr}=k_{vf}Z$, M_{fr} = const;
for shovel and screw: P_{tr}= const, M_{fr} = const.

In the suggested dependencies, the coefficient k_{vf} takes into account the change in vertical force on the excavating part depending on the depth of drilling.

The control of the movement of the excavating part is carried out by changing the supply force, and therefore ω = const.

By integrating the equation of the system we obtain:
for the case $P_{tr}=k_{vf}Z$, M_{fr} = const

$$\begin{cases} V = 2\sqrt{\frac{(Q+mg)Z-(A\alpha_z h+k_b+k_\delta+k_{vf})Z^2)}{m}}; \\ M_t = B\alpha_z Z \cdot R + \mathrm{M}_{fr}. \end{cases} \tag{3}$$

In the second case $P_{тр}$= const, $M_{тр}$ = const:

$$\begin{cases} V = 2\sqrt{\frac{(Q+mg-\mathrm{P}_{tr})Z-(A\alpha_z h+k_b+k_\delta)Z^2)}{m}}; \\ M_{\text{кр}} = B\alpha_z Z \cdot R + \mathrm{M}_{fr}. \end{cases} \tag{4}$$

When transportation of ground by screw transporter or elevator the values k_b and k_δ are equal to 0 and dependencies have the form:

$$\begin{cases} V = 2\sqrt{\frac{(Q+mg+\mathrm{P}_{tr})Z+A\alpha_z hZ^2}{m}}; \\ M_{\text{кр}} = B\alpha_z Z \cdot R + \mathrm{M}_{fr}. \end{cases} \tag{5}$$

At the stage of mathematical modeling of the earth-moving equipment operation mode, the following parameters are considered as optimal criteria: minimum energy consumption E_{cons}; maximum permissible values of supply force Q and rotation speed of the excavating part; maximum drilling per tool or minimum wear; maximum efficiency, resistivity of different patterns, etc.

The specific energy intensity E_{sp} of the process is the parameter that is also known, it is often used to compare the energy efficiency of machines.

When choosing a particular criterion of optimality, we proceed from the economic considerations of the existence of an extreme in this criterion from the mode parameters, as well as from the possibility of technical implementation of the control system with the chosen criterion of optimality. To justify the criterion of optimum of the drilling process by the excavating part, functional dependencies between the above parameters (where possible) will be determined. It is convenient to establish functional relationships between parameters using the value of specific energy intensity of the process, which is the ratio of total power N_0 and drilling efficiency E_{dr} [5]:

$$E_{dr} = \frac{N_0}{P_d}, \tag{6}$$

where N_0 – the total power;
E_{dr} - drilling efficiency

The total power is determined by the following formula:

$$N_0 = M_t\omega + QV, \tag{7}$$

Drilling efficiency:

$$P_d = jV, \tag{8}$$

where j - proportionality coefficient between the drilling efficiency and the drilling speed.

Then:

$$E_{dr} = \frac{\mathrm{M}_t\omega+QV}{jV} = \frac{\mathrm{M}_t\omega}{jV} + \frac{Q}{j}. \tag{9}$$

Parameters used as criteria for optimality of drilling process or controlled values can be determined on the value of specific energy intensity. In this regard, specific energy intensity is a general calculated criterion for the optimality of the drilling process.

The specific energy intensity E_{sp} has the structure that corresponds to the operations of the drilling process.

As a rule, specific energy intensity is used in the quantitative analysis of the operation process of machines and mechanisms. No analytical study of specific energy intensity was carried out with subsequent determination of optimal parameters. The relationship of specific energy intensity with the parameters of the drilling process allows determining their optimal values in analytical way.

All these considerations made it possible to accept the specific energy intensity as a criterion for the optimality of the operation mode of drilling and milling machines at this stage of the study.

2. Results and discussion

As a result of the study of the obtained mathematical models, it is possible to determine the dependencies connecting the supply speed, supply forces, drilling depth, resistance to motion in the clay mortar, resistance to transportation of ground and its cutting.

Also, the results of research made it possible to design the excavating parts of earth-moving machines that use the "wall in the ground" method in construction.

One of such excavating parts is mounted drilling equipment ОПН-1.50 for both trenches and boreholes (Figure 1).

The drilling equipment ОПН-1.50 is mounted excavating part to ЭО-5122А excavator. Its components are executive element 1, column 2, polyspastic system 3, control system 4 (Fig. 3) [6].

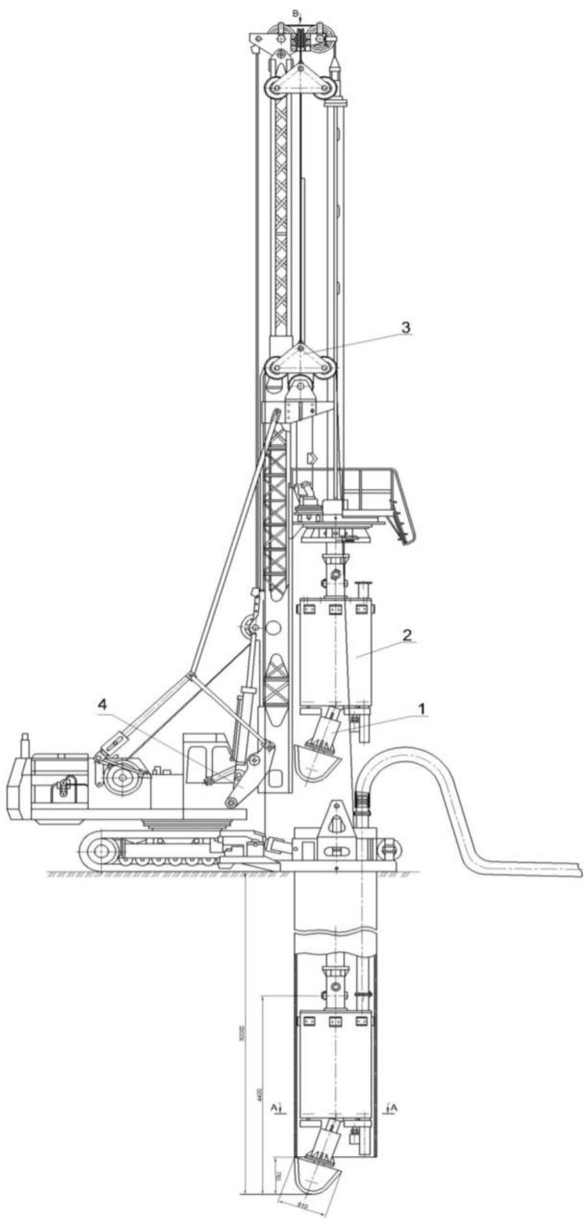

1 - executive element; 2 - column; 3 - polyspastic system; 4 - control system

Fig. 3. – Mounted drilling equipment

Executive element ОПН-1.50 equipment consists of cutting bit 1, spacer 2, handle 3, planetary reducer 4, hydraulic motor 5, hydraulic cylinder 6 (Fig. 4).

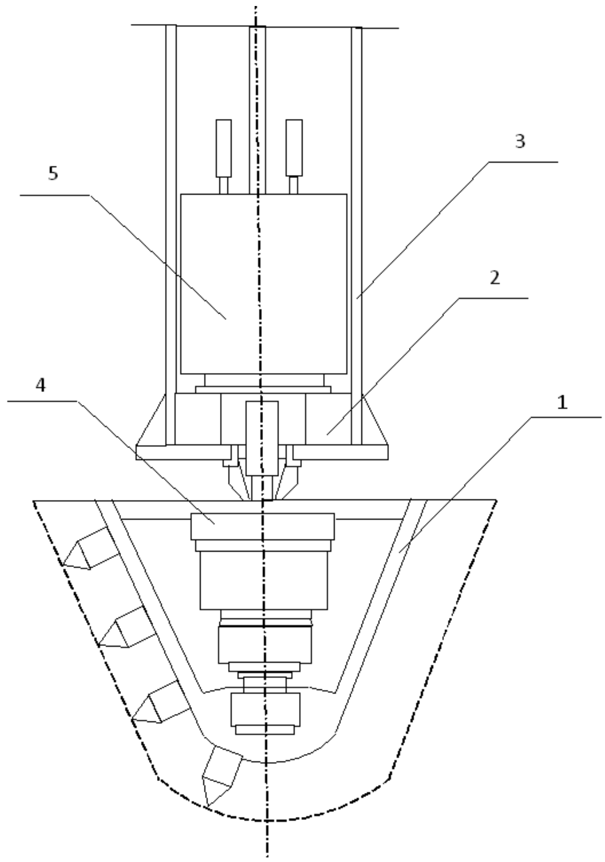

1 - crown; 2 - spacer; 3 - handle; 4 - planetary reduction gear box; 5 - hydraulic motor

Fig. 4. - Executive element of OPN-1.50 equipment

The cutting crown of the executive element of the drilling equipment is borrowed from GPK drilling combine. It is equipped with cutters of PKC type. Planetary reduction gear is arranged in cutter column concavity. A flange is welded at the base of the cutting column, which is attached to a rotating part of the planetary reduction gear.

The novelty of equipment OPN-1.50 lies in the fact that when extension of rod with hydraulic cylinder the bit deviates from vertical thereby increasing diameter of the well. This makes it possible to have one machine for drilling wells of different diameters.

Ground development during drilling by translational movement of the excavating part is carried out by appropriate ground-breaking heads. Ground-breaking head is connected with flange of the bracket, which is connecting element of the excavating part to the handle of excavator. The structural parameters of the bracket satisfy the condition of interchangeability of mountable equipment.

3. Conclusion

The block scheme of resistance forces to the motion of excavating parts of earth-moving machines has been developed, including blocks for resistance to cutting and transportation of grounds. The blocks for dry face cutting resistance include auger, shovel, screw, elevator; in terms of cutting resistance under clay solution - auger, ladle, screw, elevator, airlift, ground pump. The intersection of multiple sets of resistance forces determined the possibility of developing four mathematical models of the motion of excavating parts of drilling and milling machines.

As a result of the study of the obtained mathematical models, dependencies are determined that relate the supply speed, supply intensity, drilling depth, resistance to motion in the clay mortar, resistance to transportation of ground and its cutting.

The optimal parameters of the mode are determined according to the criterion specific energy intensity, which is the ratio of total power to drilling efficiency.

4. References

[1] Kadyrov A.S., Zhunusbekova Zh.Zh., Kyzylbayeva E.Zh., Balabekova K.G. Development and study of a mathematical model of the motion of milling working parts of earth-moving machines. The Republican Journal of University Proceedings, Karaganda: KarSTU, 2019, № 4 (77). - P. 74-78.

[2] Kadyrov A.S. Theoretical bases of design and calculation of drilling and milling earth-moving machines. Monograph. Karaganda: Sanat-Polygraphia, 2010. – 220 p.

[3] Kurmasheva B.K., Kadyrov A. S., Theory of Pre-Design. On the Exemple of Earthmoving Machines. Monograph, Karaganda, KSTU, 2019.

[4] Zhunusbekova Zh.Zh., Kadyrov A.S. Study of digging machine flat element loading in clay solution // Scientific Bulletin of National Mining University Scientific and technical journal. - Dnepropetrovsk: State Higher Educational Institution "National Mining University", 2016. – № 2(152). - P. 30-34.
[5] Kadyrov A.S., Ganyukov A.A., Zhunusbekova Zh.Zh. Calculation of the strength of the milling tool of the earth-moving machine working in clay solution//Bulletin SibADI. - Omsk, 2015. - Is.44, №4. - P. 125-130.
[6] Innov. pat. 31163 RK. Equipment for drilling wells of varying diameter/A.S. Kadyrov, Zh.Zh. Zhunusbekova, S.M. Serikov, Zh. K. Omarov; publ. 23.09.2015, Buhl. №5. – 3 p.

Information of the authors

Kadyrov Adil Suratovich, doctor of technical sciences, professor of the department "Transport Engineering and Logistics Systems" Abylkas Saginov Karaganda Technical University
E-mail: adil.suratovich@gmail.com

Zhunusbekova Zhanar Zhumashevna., PhD, acting assistant professor of the department "Transport Engineering and Logistics Systems" of Abylkas Saginov Karaganda Technical University
E-mail: zhzhzh_84@mail.ru

Ganyukov Alexander Anatolievich, PhD, acting assistant professor of the department of "Mechanics" of the Abylkas Saginov Karaganda Technical University named after
E-mail: a.ganjukov@kstu.kz

DOI 10.52209/2706-977X_2021_1_9 IRSTI 55.03.14 UDC 631.363.21

Nitrogening Hammers of the Grain Crusher of the Aknar Poultry Factory

Portnov V.S. [1], **Yurov V.M.** [2], **Makhanov K.M.** [2], **AmangeldikyzyA.** [1*], **Kopobayeva A.N.** [1]
[1]Karaganda Technical University, Karaganda, Kazakhstan
[2]Karaganda University E.A. Buketov, Karaganda, Kazakhstan
*corresponding author

Abstract. In this work, the hardening of grain crusher hammers was carried out using low-energy irradiation in a nitrogen atmosphere. Based on the use of ion-plasma nitriding, it can be concluded that additional bombardment with gas ions makes it possible to radically change the structure of the condensate by means of its surface hardening.

Keywords: hardening, irradiation, nitriding, surface.

1. Introduction

The process of preparing compound feed is associated with a number of operations for the processing of raw ingredients. The quality of compound feed is influenced by the mode of crushing of raw materials. This is the most energy-consuming and labor-intensive operation, regulated by the requirements of GOST and zootechnical recommendations, and according to average statistical data it is about 60% of the total labor costs in the procurement and preparation of feed [1]. When grinding compound feed, it is necessary to achieve a uniform composition of granules of crushed raw materials, which affects its quality.

In the feed industry and farms, the main grinding machine is the hammer crusher. It is simple in design and does not impose high requirements for operation (Fig. 1), but when grinding the feed components in it, a product is obtained in which there are under-ground particles and a significant content of dust-like fraction. Despite its simplicity, the hammer crusher does not fully meet the increased modern requirements for energy efficiency and quality of finished products obtained in the grinding process [2-4] (see theses [1-4] and the bibliography therein).

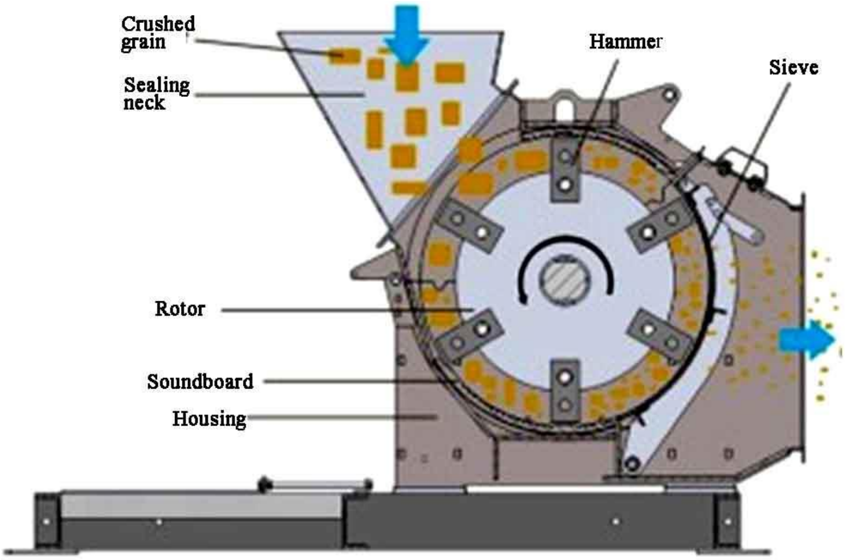

Fig. 1. - Hammer crusher

Basically, hammer crushers are applied to materials with a small to medium safety margin. The hammer mill does not process sticky or viscous materials. For all its advantages, hammer crushers have a number of disadvantages:

1. High wear rate of crushing hammers (crushing abrasives increases the likelihood of premature wear).
2. Wear of grates when processing substances with a moisture content of more than 15 percent.
3. In case of accidental loading of materials that are not completely crushed into the apparatus, damage to the main components and assemblies of the hammer crusher is possible.

To extend the life of the crusher hammers, they need to be hardened. A huge number of works are devoted to this, among which we mention some of them [5, 6]. The Aknar factory uses crusher hammers made of st-3 steel. The hardening of these steels is carried out mainly by the nitriding method [7, 8]. Analysis of modern literature has shown that ion nitriding is one of the most common methods of surface hardening of parts and tools, the use of which in industrialized countries is constantly expanding instead of various methods of chemical-thermal treatment of tools, which is environmentally harmful.

2. Experimental technique

A plasma source "PINK" with a combined heated and hollow cathode [9], developed at the Laboratory of Plasma Emission Electronics (LELP), ISE SB RAS, was used as a gas plasma source (Fig. 2). The "PINK" plasma generator is located on the upper flange of the NNV-6.6I1 chamber. The "PINK" gas plasma source is a plasma source based on a non-self-sustaining arc discharge with a combined heated and hollow cathode. On the flange 6 are mounted two water-cooled electric leads 3 for feeding the direct-heated cathode 2. A cylindrical shield electrode 1 with a diameter of 90 mm and a length of 350 mm is fixed on the vacuum side of the flange 6. The cathode is made of tungsten wire 125 mm long and 1.5 mm thick. The filament is powered by a transformer with variable (50 Hz) voltage regulation across its primary winding. The discharge is powered from a voltage source, which includes a three-phase transformer and a rectifier. The plasma source is isolated from the installation housing and is at floating potential. Gas is supplied to the gas plasma source through the gas inlet on the flange 6 from the gas inlet system, which includes two RRG-10 gas flow rate regulators.

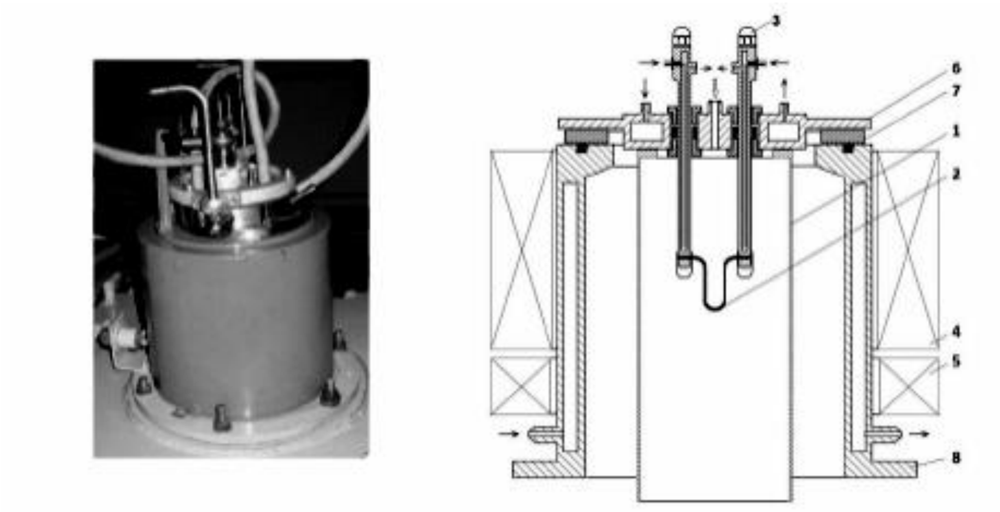

a) b)

1 - cathode cavity; 2 - heated tungsten cathode; 3 - electric input; 4 - stabilizing coil; 5 - focusing coil; 6 - water-cooled flange; 7 - insulator; 8 - water-cooled housing.

Fig. 2. - Appearance (a) and schematic diagram (b) of the plasma source "PINK"

The PINK gas plasma source [9, 10] works according to the following principle. After gas supply, pressure stabilization in the chamber and creation of a longitudinal magnetic field with magnetic induction B = 0.1–3 mT in the working volume of the plasma generator, the cathode is heated and voltage is applied to the electrodes of the discharge system. The electrons emitted by the hot cathode are accelerated towards the additional electrode, which at the moment of discharge ignition acts as an auxiliary anode, and ionize the gas in the cathode cavity, thereby provoking the ignition of the discharge in the gap between the heated cathode and the ignition electrode. In this case, the hollow cathode is filled with plasma, which propagates into the vacuum chamber. This leads to switching the combustion of the discharge to the main anode (inner walls of the vacuum chamber), i.e. the main non-self-sustaining arc discharge is ignited. Under the influence of an external magnetic field, the trajectory of electrons emitted from the heated cathode is bent. The movement of electrons occurs in a cylindrical spiral, which increases their path to the anode, thereby increasing the efficiency of gas ionization.

By varying the filament current, and hence the emission of electrons from the hot cathode, one can easily control the discharge current from tens to hundreds of amperes at a combustion voltage of several tens of volts. Such a discharge is classified as a non-self-sustaining hot-cathode arc discharge without a cathode spot. This arc discharge will make it possible to generate low-temperature plasma in volumes ($\geq$0.1 m^3) with a concentration of ne ~ 10^9–10^{11} cm^{-3} and a uniformity of ± 15% of the average value.

The technological mode of the nitriding process of the crusher hammers is presented below.

Preliminary preparation:

1. Degreasing of hammers with Nefras C2-80/120 (Fig. 3a).

2. Cleaning and polishing in the bath of the EPP-40 electrolytic-plasma polishing unit (Fig. 3b), with the following parameters: the composition of the polishing solution is a 5% aqueous solution of ammonium sulfate; solution temperature - 850 ºC; cathode-anode voltage 300 V, current 40 A; processing time 5 min.

3. After unloading from the EPP-40 bath, the hammers are washed with running water and treated with steam using a steam jet device UPS 4.3-geyser (Fig. 3c).

4. After steam-jet cleaning, the hammers are wiped with coarse calico moistened with alcohol and placed in an oven for drying and preheating to 1500 ºC.

a) b) c)

Fig. 3. - Degreasing of hammers with Nefras S2-80/120 (a), polishing in the bath of the EPP-40 unit (b), steam jet device UPS 4.3-geyser (c)

Ion-plasma nitriding process:

1. Prepared hammers are installed in the vacuum chamber of the NNV 6.6-I1 installation (Fig. 4 a) using special equipment in the center of the rotating table (Fig. 4 b).
2. Forevacuum pumping of the installation chamber is carried out to a pressure of 1Pa (time is about 15 min.).
3. Further evacuation of the chamber is carried out by a high-vacuum diffusion pump up to a pressure of $5*10^{-3}$ Pa. (time 20-25 min.).
4. Then, argon is injected into the chamber through the gas leak and with the help of the BUEN electromagnetic leak control unit the pressure in the chamber is maintained at $2*10^{-1}$ Pa.

a) b)

Fig. 4. - Vacuum chamber of the NNV 6.6-I1 installation (a), special equipment in the center of the rotating table (b)

5. To carry out the process of ionic cleaning and heating, a plasma source with a heated PINK cathode is switched on, a heating current of 120 A and an ion current of 5 A are set.
6. The reference voltage block turns on and the bias voltage of -1000 V is applied to the parts. To eliminate the formation of micro arcs on parts, the reference voltage unit operates in a pulsed mode with a frequency of 25 kHz and a duty cycle of 80 %.
7. The table rotation drive is switched on and the rotation speed is set to 5 rpm.
8. Within 5-7 minutes, the PINK ion current is gradually brought to 45-50 A, while the heating of the hammers is monitored using a Smotrich 7 pyrometer focused on the part through the viewing window of the chamber.
9. When the temperature reaches 450 ºC (time 20-25 min.), Nitrogen of special purity is admitted into the chamber through a parallel gas main, with the help of an RRG-10 flow meter (nitrogen flow rate is set at 2 l /min.), The pressure is maintained at the level of $1.8\text{-}2.2*10^{-1}$ Pa. Thus, the regime of ion-plasma nitriding of parts in an argon-nitrogen gas mixture is established. Further, throughout the entire process, the temperature of the products is monitored, if necessary, adjusting the PINC current and the reference voltage. The nitriding process lasts 3 hours, after which the products are allowed to cool in a vacuum chamber for an hour and unloaded.

The results of measurements of the microhardness of the hammer surface using an HV-1000 microhardness tester with a load on the indenter of 1 kg gave the following results: before nitriding about 154,4 HV, after about 449 HV (Fig. 5).

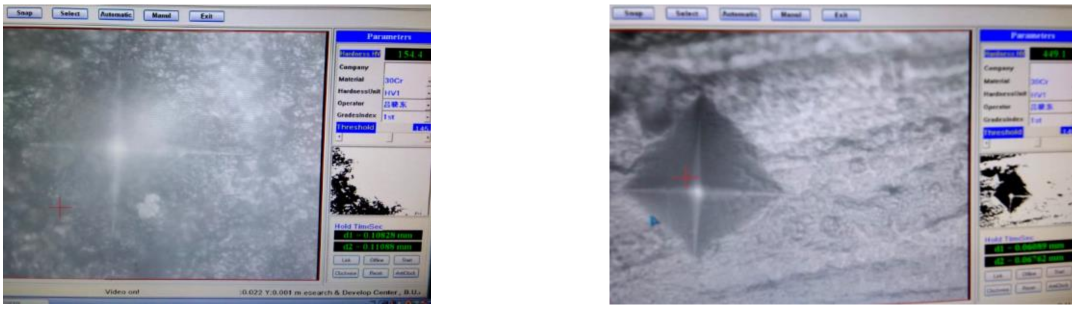

a) b)

Fig. 5. - Microhardness of the surface of hammers before (a) and after (b) nitriding

Thus, by increasing the surface hardness of the hammers, the service interval of the hammer crusher can be significantly extended.

3. Discussion of experimental results

PINK Assistance shows that the structure of the coating can be changed using ion bombardment. In fig. 6 shows an image of a TiN coating after exposure to nitrogen.

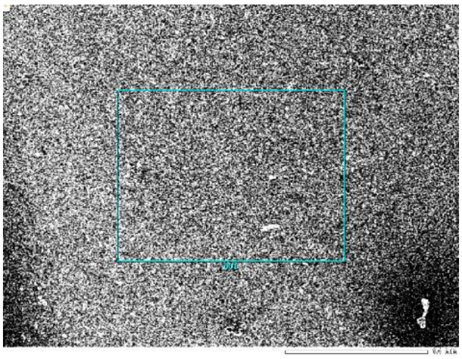

Fig. 6. - Electron microscopic image of TiN coating after hammer ion bombardment

One of the promising methods of assisting the coating synthesis process is low-energy ion irradiation [11-13], during which there is no significant change in the coating/substrate system, but it becomes possible to regulate the structural-phase and elemental composition of coatings and their properties.

It was shown in [13] that the simultaneous irradiation of titanium with nitrogen ions, first, excludes the formation of high-energy nano- and submicrocrystalline substructures with a high curvature of the crystal lattice and a high density of partial disclinations in grain boundaries and associated high local stresses, and - second, it stimulates the epitaxial mechanism of the formation of the nitride phase on the γ-austenite substrate, and third, it leads to an increase in the plasticity of the nitride coating (from 3 to 6 %).

Plasma assistance can be used in vacuum-arc deposition of coatings, which is one of the stages of complex processing of steels [14-16], including preliminary ionic nitriding of the surface and subsequent application of a TiN coating in a single technological cycle. Such a combined treatment of steel 40X allows the formation of a nitride (γ′-Fe4N) in the surface layer and provides a gradient decrease in hardness along the depth of the sample. This provides an increase in the adhesion of the TiN coating to the steel substrate and a significant increase in the wear resistance of the obtained composition.

In [16], experiments on the deposition of TiN coatings by a vacuum-arc plasma-assisted method are shown at a gas plasma generator current of 10^{-12} A and an arc evaporator current of 50–100 A, in which the effect of negative bias voltage on the formation of ion-plasma coatings was studied. the value was 15, 200, 600, and 1000 V. It was found that during plasma-assisted coating deposition, the bias voltage applied to the sample is of decisive importance in changing the structure and phase state during the formation of the layer. Studies have shown that at small negative values of the displacement stress, a lamellar structure with a high level of elastic stress fields is formed. An increase in the bias leads to the formation of a nanosized polycrystalline structure in the wafers as a result of splitting into separate disoriented crystallites. The optimal bias voltage turns out to be $U_{cm} = -200$ V. It is assumed that the modification of the structure and properties of TiN deposited under vacuum-arc sputtering of titanium under irradiation with low-energy nitrogen ions is due to the development of relaxation processes due to ion mixing, generation of point defects, and an increase in the diffusion mobility of adatoms on growing surface.

The results of measurements of the microhardness of the hammer surface using an HV-1000 microhardness tester with a load on the indenter of 1 kg gave the following results: before nitriding about 150 HV, after nitriding about 450 HV, after spraying TiN about 900 HV.

4. Conclusion

Ionic nitriding (3 hours) using a plasma source "PINK" with a combined heated and hollow cathode instead of chemical-thermal treatment of crusher hammers (10-14 hours) increases their service life by 3 times. This leads to an increase in the energy efficiency of crushers and an increase in the resource of grain grinding. Spraying hammers with a titanium nitride coating leads to a 6-fold hardening of the hammers, but the cost of TiN coating is much higher than ion nitriding and can be used in some cases.

5. Acknowledgments

The work was carried out under the program of the Ministry of Education and Science of the Republic of Kazakhstan Grant No. 0118RK000063.

6. References

[1] Palkin A.V. Improving the efficiency of the hammer screenless feed crusher: dis. Cand. tech. sciences. - Kirov, 2000. - 160 p.

[2] Rybalkin D.A. Improving the efficiency of the process of grinding the husk of cereals and oilseeds by modernizing the hammer crusher: dis. Cand. tech. sciences. - Saratov, 2018. - 160 p.

[3] Lopatin L.A. Increasing the efficiency of the process of grinding grain by improving the working bodies of the hammer crusher: dis. Cand. tech. sciences. - Kirov, 2018. - 185 p.

[4] Mironov K.E. Increasing the efficiency of the process of grinding grain with the substantiation of the parameters of the working bodies of the impact crusher: dis. Cand. tech. sciences. - Knyaginino, 2018. - 142 p.

[5] Yalpachik F.E., Yalpachik G.S., Kryzhachkovsky N.L., Kyurchev V.N. Feed grinders: design, calculation. - Zaporozhye "Коммunar", 1992. - 292 p.

[6] Chudina O.V., Gladova G.V. The choice of materials and methods for hardening parts of transport engineering. - M.: MADI, 2015. - 120 p.

[7] Gerasimov S.A., Kuksenova L.I., Lapteva V.G. Structure and wear resistance of nitrided structural steels and alloys. - M.: Publishing house of MSTU im. N.E.Bauman, 2012. - 518 p.

[8] Ramazanov K.N. Investigation of structural-phase transformations and properties of surface layers of steels during ion nitriding in a low-pressure glow discharge: dis. doctor tech. sciences. - Ufa, 2015. - 332 p.

[9] Grigoriev S.V., Koval N.N., Tolkachev V.S. Low-pressure arc discharges with a hollow cathode and their application in plasma generators and sources of charged particles // Izvestiya VUZov. Physics. - 2001. - T. 44. - No. 9. - P. 28–35.

[10] Korosteleva E.N., Pribytkov G.A., Gurskikh A.V. Investigation of the structure and properties of sintered titanium – copper materials // Physical Mesomechanics. - 2004. - T. 7. - Special issue. - Part 2. - P. 75–77.

[11] Borisov D.P., Shchanin P.M., Koval N.N. Generation of bulk plasma by an arc discharge with a heated cathode // Izvestiya VUZov.. Physics. - 1994. - T. 37. - No. 3. - P. 115-121.

[12] Vintizenko L.G., Grigoriev S.V., Koval N.N., Tolkachev V.S., Lopatin I.V., Shchanin P.M. Hollow cathode low pressure arc discharges and their application in plasma generators and charged particle sources. // Izvestiya VUZov. Physics. 2001. - T. 44. - No. 9. - P. 28-35.

[13] Tyumentsev A.N., Korotaev A.D., Pinzhin Yu.P. et al. Influence of low-energy ionic irradiation on the microstructure of titanium nitride coatings. // Surface. X-ray, synchrotron and neutron research. – 1998. - No. 10. - P. 92-100.

[14] Goncharenko I.M., Grigoriev S.V., Lopatin I.V. et al. Surface modification of steels by complex diffusion saturation in low pressure arc discharge. // Surface and Coatings Technology. – 2003. - V. 169-170. - P. 419-423.

[15] Borisov D.P., Goncharenko I.M., Koval N.N., Schanin P.M. Plasma-assisted deposition of a three-layer structure by vacuum and gas arcs. // IEEE Transactions on Plasma Science. – 1998. - V. 26. - № 6. - P. 1680-1684.

[16] Goncharenko I.M. Complex modification of steels and TiN coatings in plasma of low pressure arc discharges: dis. Cand. tech. sciences. - Tomsk, 2004. - 168 p.

Information of the authors

Portnov Vasily Sergeevich, doctor of technical sciences, professor of the department of “Geology and Exploration of Mineral Deposits”, Karaganda Technical University
E-mail: vs_portnov@mail.ru

Yurov Viktor Mikhailovich, Ph.D., phys.-math. sciences, associate professor, E.A. Buketov Karaganda University
E-mail: exciton@list.ru

Makhanov Kanat Matovich, Candidate of phys.-mat. sciences, associate professor EA. Buketov Karaganda University
E-mail: makhanov_kanat@mail.ru

Amangeldikyzy Altynai, PhD, teacher of the department “Geology and exploration of mineral deposits” of Karaganda Technical University
E-mail: amangeldykyzy@inbox.ru

Kopobaeva Ayman Nygmetovna, senior teacher of the department “Geology and exploration of mineral deposits” of Karaganda Technical University
E-mail: a.kopobaeva@kstu.kz

DOI 10.52209/2706-977X_2021_1_14 **IRSTI 55.0.07** **UDC 621.225.4**

Determination of the Functional Accuracy of the Piston Pair of Axial Hydraulic Machines

Kyzyrov R.B., Bondarev I.A, Sinko A.N., Nikonova T.Yu.*
Karaganda Technical University, Karaganda, Kazakhstan
*corresponding author

Abstract. The article deals with the problems of establishing dependencies for determining the functional geometric parameters of a piston pair of axial-piston hydraulic machines.The hydraulic drive is increasingly used in all sectors of the national economy, including in various branches of mechanical engineering. The widespread introduction of hydraulic transmissions is caused by their advantages over other types of transmissions: a wide range of stepless speed control of working bodies, low inertia, low specific weight per unit of power, high efficiency, the ability to perceive significant loads. One of the main elements of the hydraulic drive is a pump, the reliability and durability of which largely depends on the performance of the entire hydraulic drive.

Keywords: hydraulic drive, axial piston machine, liquid leakage, piston pair, functional accuracy.

1. Introduction

The hydraulic drive is increasingly used in all sectors of the national economy, including in various branches of mechanical engineering. The widespread introduction of hydraulic transmissions is caused by their advantages over other types of transmissions: a wide range of stepless speed control of working bodies, low inertia, low specific weight per unit of power, high efficiency, and the ability to perceive significant loads. One of the main elements of the hydraulic drive is a pump, the reliability and durability of which largely depends on the performance of the entire hydraulic drive.

At present, volumetric hydraulic machines, including piston pumps and, above all, axial - piston pumps, are widely used in mechanical engineering. Axial-piston pumps are compact, high energy consumption per unit weight and simple design. Their widest distribution was facilitated by such qualities as high characteristics in terms of mass and overall dimensions, insignificant power losses and a small amount of the moment of inertia of the rotating masses.

One of the ways to improve the performance of piston machines is to determine the optimal gaps in the friction pairs, in particular, between the pistons and the holes in the cylinder block. The size of the design gap between the piston and the housing is chosen from two mutually contradictory requirements: ensuring a minimum amount of friction, small leaks and high efficiency.

Fluid leaks through the gap between the piston and the cylinder, along with leaks through the distribution system, the spherical piston joint and the hydrostatic shoe, refer to direct external leaks. They depend on the magnitude of the discharge pressure, affect the feed rate and in different types of axial-piston hydraulic machines have a different role on their characteristics. The amount of liquid leakage through the gaps depends on the temperature of the liquid, is inversely proportional to its viscosity and is directly proportional to the value of the pressure drop.

The smallest gap value depends on the coefficient of linear expansion of the cylinder block and piston materials, the operating temperature range, the manufacturing accuracy of the mating surfaces, and the working fluid. However, reducing the gap can lead to jamming of the pistons in the holes of the cylinder block when changing the operating temperature of the hydraulic drive.

Thus, temperature changes in the dimensions of the mated parts are essential for the operation of the pump pistons: strong heating of the pistons with small gaps can cause a sharp decrease in the gaps and jamming; a significant increase in the gaps causes a sharp increase in fluid leakage and deterioration of the hydraulic drive. In addition, the situation is complicated by the fact that the piston is heated more than the cylinder, and they are often made of different materials with different linear expansion coefficients. The use of various materials is explained by the desire to reduce the amount of wear of the friction pair. In connection with the above, the definition of optimal gaps is an ambiguous and contradictory problem, the solution of which is devoted to this work.

2. Results and discussion

Improving the quality of hydraulic machines can be achieved not only by improving their designs, using new technological processes and materials, but also by using the principles of functional interchangeability. Functional interchangeability helps to obtain stable values of the output parameters of the machines.

In modern technologies of dimensional processing, the transition from dimensional standardization to functional standardization is carried out for the performance of certain functions by the product, depending on the accuracy of the functional parameters. To perform the service purpose of the product in a working state, the functional boundaries of the parameters are determined, the difference between which determines the functional tolerance. The accuracy is normalized according to the value of this tolerance, followed by its distribution from the upper level (product) to the final part of the lower level.

In mechanical engineering, the modern concept of accuracy is considered in four aspects: functional, design, technological and metrological. Accordingly, there are functional, design and technological tolerances. Functional tolerances are set based on the reliable operation of the machine in accordance with the functional limits of the parameters.

The functional tolerance T_f is equal to the difference between the largest L_f ^ max and the smallest L_f^min permissible parameter values, determined taking into account the permissible change in the operating parameters of the machine, i.e., the permissible functional deviations. The functional tolerance T_f includes the operational T_ec and the design T_c tolerances. The operational tolerance characterizes the margin of accuracy that ensures the preservation of the required functional properties of the product during operation. The design tolerance takes into account the manufacturing errors of parts, joints, and the product as a whole.

The design aspect of accuracy is associated with the implementation of the functional aspect, i.e., with the determination of the accuracy of the geometric shapes of parts and their relative position. So, in this case, the hydraulic circuit is a functional aspect, the hydraulic drive that implements this scheme is a design aspect. Design tolerances are also related to the functional (service) purpose of the machine and its working conditions. They are installed on the basis of an analysis of the operation of the machine, taking into account the costs of its manufacture and subsequent operation.

The tolerances for intermediate dimensions that arise during the technological process are called technological. They are associated with the resulting errors and have many values in accordance with the construction of a specific technical process for manufacturing parts.

The metrological aspect of accuracy is associated with the solution of the problem of the maximum approximation of the estimated value of the parameter to its actual value. This requires continuous improvement of methods and controls up to the nano-dimensional level.

Figure 1 shows the layout of the tolerances for a single surface (size) of the part, based on the functional aspect of accuracy.

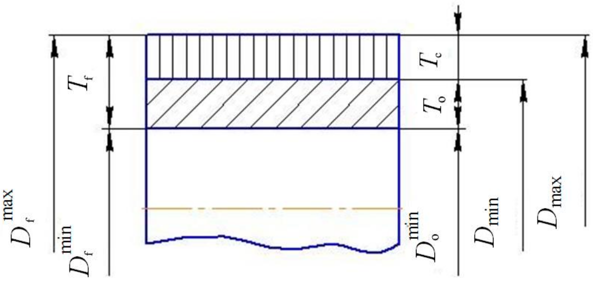

Fig. 1 - Layout of the tolerance fields of the covered part

The design tolerance T_c characterizes the accuracy of the nominal size of the part and is equal to the difference between the largest Dmax and the smallest Dmin dimensions of the part in accordance with the design drawing, i.e. this is the reference value of the accuracy of the part size. The design tolerance includes errors in the manufacture of parts, and in the case of a mating surface, in addition, it takes into account errors in the assembly of joints, their adjustment, and also compensates for other errors. Design tolerances also correspond to the functional (service) purpose of the surface of the part, the purpose of the part itself and the conditions of its operation. They are installed on the basis of an analysis of the operation of the machine, taking into account the costs of its manufacture and subsequent operation. This also takes into account the technological performance of the machine, the connection and the part itself, i.e., the cost-effectiveness of achieving a given accuracy in the manufacturing process of the part is analyzed. In this sense, there is a relative relationship between design tolerances and technological tolerances.

The operational tolerance T_o ensures the preservation of the required functional properties in the conditions of possible changes occurring in the machine during operation, and therefore is associated with changes in the accuracy of parts and connections. For example, it can take into account the temperature deformations of parts, surface wear, etc. In general, the phenomena underlying the formation of the operational tolerance have a different effect on its value, both in absolute value and in direction.

For the parts covered, the maximum functional size D_f^{max} is equal to the maximum design size Dmax. The minimum functional D_f^{min} corresponds to the minimum operational size D_o^{min}.

When the size exceeds the limits of D_o^{min}., the corresponding part (connection) enters a state in which the product is not able to perform the specified functions, while maintaining the values of the specified parameters within the limits set by the regulatory and technical documentation, i.e., it loses its operability.

Figure 2 shows the layout of the tolerances of the piston pair of the axial-piston hydraulic machine. The functional tolerance of each element of the pair is equal to the sum of the design T_c and operational T_o tolerances:

$$T_f = T_c + T_o = T_c + T_t + T_p \tag{1}$$

where T_t is the tolerance for the temperature deformation of the element: T_p is the tolerance for the deformation of the element as a result of the pressure drop.

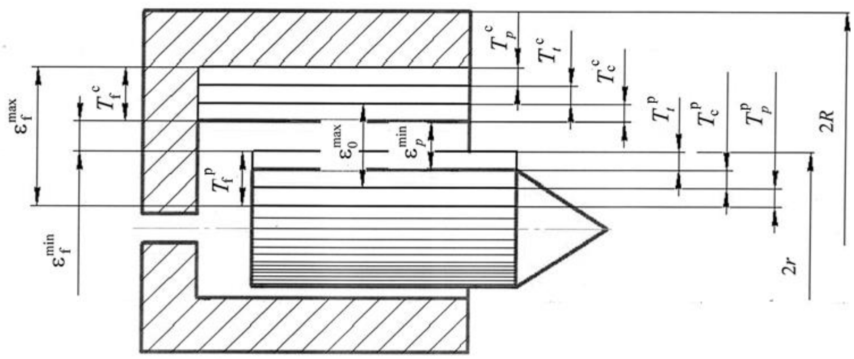

Fig. 2. - The layout of the tolerances of the piston pair of the axial-piston hydraulic machine

The initial gap ε_0 in the piston pair is determined in the non-working state of the hydraulic machine. It is formed by the constructive accuracy of the coupling and can take values from ε_0^{min} to ε_0^{max}within the design tolerances. Functional gaps ε_f are formed during the operation of the hydraulic machine. As a result of temperature deformation, depending on the material of the elements of the piston pair, the minimum functional gap ε_f^{min}can be either greater or less than the initial structural gap ε_f^{min}. The increase in the gap due to the pressure drop should be taken into account at high working fluid pressures in the hydraulic system, up to 100 MPa or more.

Thus, the radial clearance in the piston pair of an axial-piston hydraulic machine, taking into account changes in pressure and temperature, can be determined by the formula:

$$\varepsilon = \varepsilon_0 + \Delta\varepsilon_t + \Delta\varepsilon_p \tag{2}$$

where ε_0 is the design gap, based on the design accuracy of the coupling;

$\Delta\varepsilon_p$ and $\Delta\varepsilon_t$ is the change in the gap as a function of the temperature and pressure of the working fluid, respectively.

The change in the gap due to the heating of the elements of the piston pair can be determined by the formula:

$$\Delta\varepsilon_t = d\beta(t_K - t_0) - \alpha(t_n - t_0)] \tag{3}$$

where d is the diameter of the piston;

β and α are the coefficients of thermal expansion of the material of the housing (sleeve) and the piston;

t_C *and* t_n are the average temperatures of the housing and the piston; t_0 is the initial initial temperature at which the design gap was obtained according to the design tolerances T_c^c and T_c^p.

Since there are difficulties in determining the average temperatures t_C and t_p, the calculation of the gap change $\Delta\varepsilon_t$ can be carried out using a simplified formula:

$$\Delta\varepsilon_t = d\Delta\alpha\Delta t \tag{4}$$

where $\Delta\alpha = \alpha_K + \alpha_n$ the difference between the coefficients of linear expansion of the materials of the mating parts of the body (α_K) and piston ($\alpha_П$) values, which are an average temperature of +20 °C;

$\Delta t = t - t_0$ the difference between the temperature of the material related parts ($t_K = t_n = t$, slow heating or cooling) and the original (initial) temperature.

The change in the gap in the piston pair from the action of the pressure of the working fluid can be determined similarly to the definition of the gap of a cylindrical slot:

$$\Delta\varepsilon_p = \frac{pr}{E_k}\left(\mu_k + \frac{R^2+r^2}{R^2-r^2}\right) + \frac{pr}{E_п}(1-\mu_п) \tag{5}$$

where p - is the pressure of the working fluid;

r and R are respectively, the outer radii of the piston and the housing (sleeve) of the hydraulic machine;

E_k and $E_п$ are the elastic modulus and Poisson's coefficients of the material of the housing (sleeve) and the piston, respectively.

Substituting (4) and (5) into formula (2), we obtain an expression for determining the functional gap of the piston pair:

$$\varepsilon = \varepsilon_0 + 2r\Delta\alpha\Delta t + \frac{pr}{E_k}\left(\mu_k + \frac{R^2+r^2}{R^2-r^2}\right) + \frac{pr}{E_п}(1-\mu_п) \tag{6}$$

Then the canonical formula for determining the specific leaks per unit width of the gap will take the form:

$$Q` = \frac{\Delta p\varepsilon^3}{12\mu l} \tag{7}$$

where Q is the volume of liquid flow;

Δp is the pressure drop;

μ is the absolute viscosity of the liquid; l is the length of the gap (the working part of the piston):

$$Q = \frac{\pi\Delta p\varepsilon^3 d}{12\mu l} \tag{8}$$

The calculation of the tolerances for the main geometric parameters in expression (8) can be performed in accordance with the method that assumes that, if between the output parameters of a compound y and its dimensions $x_1, x_2, \dots, x_n$ there is an analytical dependence of the form $y = f(x_1, x_2, \dots, x_n)$, and it, differentiable to n-th order for all argument values $x_1, x_2, \dots, x_n$ in between $z_1 \pm \delta_1$, $z_2 \pm \delta_2$, …, $z_n \pm \delta_n$, where $z_1, z_2, \dots, z_n$ – the partial values of the arguments corresponding to the characteristics under consideration, then the tolerance for the value y is determined from the expression:

$$\vartheta = \frac{\mu}{\rho} \tag{9}$$

where ϑ – kinematic coefficient of viscosity;

μ – dynamic viscosity index;

$$\delta y = \sqrt{\left(\frac{df}{dx_1}\right)^2_{x_1=z_1} + \delta_1 k_1^2 + \left(\frac{df}{dx_2}\right)^2_{x_2=z_2}} + \delta_1 k_1^2 + \dots + \left(\frac{df}{dx_n}\right)^2_{x_n=z_n} + \delta_n k_n^2 \tag{10}$$

where $\delta_1, \delta_2, \dots, \delta_n$ – appropriate tolerances for values $x_1, x_2, \dots, x_n$;

$k_1, k_2, \dots, k_n$ – scattering coefficients whose values are determined by the laws of the distribution of quantities $x_1, x_2, \dots, x_n$.

We define the partial derivatives of the expression for fluid leaks by functional geometric parameters.

By the diameter of the piston:

$$\frac{\partial Q}{\partial d} = \frac{\pi\Delta p\varepsilon^3}{12\mu l} \tag{11}$$

By the gap in the piston pair:

$$\frac{\partial Q}{\partial \varepsilon} = \frac{\pi\Delta p\varepsilon^3 d}{4\mu l} \tag{12}$$

Along the length of the working part of the piston:

$$\frac{\partial Q}{\partial l} = \frac{\pi\Delta p\varepsilon^3 d}{12\mu l^2} \tag{13}$$

Then, using the equation and counting $k_1 = k_2 = \dots = k_n = 1$, in the general case, we can write:

$$\delta Q = \sqrt{\left(\frac{\partial Q}{\partial d}\right)^2 \delta^2 d} + \left(\frac{\partial Q}{\partial \varepsilon}\right)^2 \delta^2 \varepsilon + \left(\frac{\partial Q}{\partial l}\right)^2 \delta^2 l \tag{14}$$

From equation (13) for $\delta\varepsilon = \delta l = 0$, using the equation (10), we obtain:

$$\delta d = \frac{12\mu l \delta Q}{\pi \Delta p \varepsilon^3} \tag{15}$$

When $\delta d = \delta l = 0$ using the equality (12):

$$\delta d = \frac{4\mu l \delta Q}{\pi \Delta p \varepsilon^3 d} \tag{16}$$

When $\delta d = \delta\varepsilon = 0$ using the equality (13):

$$\delta l = \frac{12\mu l^2 \delta Q}{\pi \Delta p \varepsilon^3 d} \tag{17}$$

Thus, the obtained expressions (15) - (17) allow us to determine the tolerances for the main functional geometric parameters of the piston pair.

3. Conclusion

Based on the principles of functional interchangeability, based on functional tolerances, an expression is established for determining the radial clearance in the piston pair of an axial - piston machine. The presented expression is obtained taking into account the initial design tolerance and operational tolerances for changing the gap depending on the temperature in the joint and the pressure of the working fluid. Expressions for determining the tolerances for the main functional geometric parameters of the piston pair are derived from the equation for accounting for fluid leaks.

The application of the principles of functional interchangeability in the design and manufacture of the main elements of the piston pair will allow a reasonable approach to the assignment of tolerances for the main geometric parameters, to assess the correctness of the assignment of tolerances, to identify the technological possibilities of interchangeability and increase the stability of the connection.

4. References

[1] Sveshnikov V. K. Machine hydraulic drives: handbook. - M.: Mashinostroenie, 2008. – 640 p.
[2] Hydraulics, hydraulic machines and hydraulic drives. - M.: Alliance, 2010. – 424 p.
[3] Hydraulics, hydraulic machines and hydropneumoprivod / T. V. Artemyeva [et al.]; ed. by S. P. Stesin. - M.: Akademiya, 2006. – 336 p.
[4] Filippova E. M. Mathematical modeling of leaks in axial-plunger hydraulic machines // Tractors and agricultural machines. - 2013. - No. 3. - p. 24-25.
[5] Semenova T. V. Investigation of the influence of friction on the stress-strain state of the piston in an axial piston pump // Friction and wear. – 2000. – V. 21, № 3. – P. 291-294.
[6] High technology machining mechanical engineering. – M.: Higher School of Economics, 2007. - 327 p.
[7] Suslov, A. G. Scientific bases of mechanical engineering technology. – M.: Mashinostroenie, 2002. - 684 p.
[8] Technology of mechanical engineering: in 2 vols. - M.: Publishing House of the Bauman Moscow State Technical University, 2001. - Vol. 1. Fundamentals of mechanical engineering technology. - 564 p.
[9] Hydropneumoautomatics and hydraulic drive of mobile machines. Volumetric hydro-and pneumatic machines and transmissions / A. F. Andreev [et al.]; ed. by V. V. Guskov. - Minsk: Vysh. shk., 1987. - 310 p.
[10] Seals and sealing equipment: handbook / L. A. Kondakov [et al.]; under the general editorship of A. I. Golubev and L. A. Kondakov. - M.: Mashinostroenie, 1994. – 448 p.
[11] Lazovetsky V. V. Hydro-and pneumatic systems of transport and technological machines /V. V. Lazovetsky. - M.: Lan, 2012. - 555 p.
[12] Sheypak A. A. Hydraulics and hydropneumoprivod. - M.: MGIU, 2005. - Part 1. Fundamentals of mechanics, liquid and gas. - 192 p.
[13] Zhukov, V. K. Theory of errors of technical measurements. - Tomsk: TPU, 2009. - 180 p.

Information of the authors

Kyzyrov Kayrolla Beisembaevich, candidate of technical sciences, associate professor of the department "Technological equipment, machine building and standardization" of Karaganda Technical University
E-mail: kyzyrov@mail.ru

Bondarev Igor Alexandrovich, undergraduate of the department "Technological equipment, machine building and standardization" of Karaganda Technical University
E-mail: bondarev_i@mail.ru

Sinko Alexander Nikolaevich, candidate of technical sciences, associate professor of the department "Technological equipment, machine building and standardization" of Karaganda Technical University
E-mail: sinko1947@mail.ru

Nikonova Tatyana Yurievna, Ph.D., acting associate professor of the department "Technological equipment, machine building and standardization" of Karaganda Technical University
E-mail: nitka82@list.ru

DOI 10.52209/2706-977X_2021_1_19 **IRSTI 55.31.29** **UDC 621.923**

Selection of Optimal Parameters for a Cutting Tool When it Comes to Machining Shaped Parts Made of Alloy Steel

Buzauova T.M.*, Smagulov A.S.
Karaganda Technical University, Karaganda, Kazakhstan
*corresponding author

Abstract: This article provides recommendations for selection of cutting tools parameters when machining of shaped parts made of alloy steel. The factors that have an effect on machining of shaped parts made of alloy steel are considered. A dependency graph of a P_z component force against the number of a milling cutter's revolutions was drawn. An experimental form of a milling cutter's sharpening for machining of alloy steel is presented. Recommendations were made to increase a tool's life which will increase machining accuracy and productivity.

Key words: cutting tool, optimal parameters, alloy steel, force dependence, rotation

1. Introduction

The products of modern mechanical engineering are characterized by the complication of the design of parts, the inclusion of free-form surfaces in them. This is directly reflected in the production of tooling, dies, molds, foundry models and similar products. When processing such parts, large volumes of cut layers are removed, associated with obtaining complex spatial shapes, as a result of which there is a decrease in the durability of an expensive tool, therefore, a decrease in the productivity of the processing process. Improving the wear resistance of cutting tools is one of the important tasks of mechanical engineering technology.

High-performance machining of shaped surfaces is a complex technological challenge. Particular difficulties are caused by the processing of precise shaped surfaces, since the access of particles of the working medium to various elements of the surface and the corresponding intensity of processing depend on the configuration of the processed parts. In blind pockets, holes, grooves and depressions, processing is slower and requires more careful selection of the size and shape of the particles of the working medium.

The processing of shaped surfaces differs from the processing of flat and other simple surfaces by a pronounced nonstationarity, the level of which has a significant impact on the choice of modes of the technological process of processing and equipment. Therefore, the choice of technology and equipment should be preceded by a thorough analysis of the patterns inherent in the process of processing shaped surfaces.

In this case it is important to select of optimal parameters for a cutting tool when it comes to machining shaped parts made of alloy steel.

2. Results and discussion

Studies [1] show that the process of machining shaped parts made of alloy steel results in wear because of chipping of carbide inserts in combination with abrasive and adhesive wear. In this context, the task is to find the optimal geometry of a milling cutter blade which will reduce wear and prevent chipping, and, therefore, to manufacture a tool with a life of its work – one part.

The shape of a blade has a great impact on a tool life. References [1, 2] have recommendations for choosing an optimal shape of a blade, depending on a number of factors, but the study is not complete and requires additional research, as well as defining internal logical connections, at least qualitative. Thus, it is essential to research and identify key design features of a milling cutter for machining shaped parts made of alloy steel.

Resultant R of these forces is the cutting force on a milling cutter tooth. The cutting force R does not remain constant throughout an arc of contact between a milling cutter tooth and a workpiece, neither in value nor in direction. As we mentioned above, when a milling cutter rotates, the cut section continuously changes from zero to the maximum value which results in continuous changes in the cutting force. In addition, due to the rotation of a milling cutter, the direction of the force *R* will also change continuously against constant directions characteristic of a milling machine, for example, against the plane of a machine table.

The cutting force *R* consist of horizontal P_s and vertical P_v. The circumferential force P_z is applied to calculate the mechanism of the main movement of a machine and the power spent on cutting. Radial force P_y causes deformation of machine parts and bending of a milling mandrel. The horizontal force P_s, the feed force, is applied to calculate the machine feeding mechanism and clamping parts of a mechanism [4]. The vertical force P_v pushes a milling cutter away from a processing workpiece.

Among all values of the resultant and its components, which they assume throughout an arc of contact, the most important are the maximum values of the circumferential force $P_{z\max}$, the feed force P_s max and the vertical force P_{ymax}, which are essential when calculating the strength of machine parts, and the average value of the circumferential force

P_{zcp} used to determine capacity consumed for cutting power. The circumferential force (H) impacting on one tooth can be defined as:

$$P_z = pf \tag{1}$$

where p – specific pressure, H/mm^2;

f – cross-sectional area of a cut taken by a given tooth. Specific pressure depends on thickness of a cut: the greater thickness, the lower specific pressure, and is defined by the formula:

$$p = C_p a^y \tag{2}$$

where C_p – coefficient for processing conditions;

a^y –value depending on the processed material, dulling of a tool and lubricant

Then the component of the cutting force P_z will be defined as:

$$P_z = pf = C_p a^y ab = C_p a^{y+1} b = C_p a \tag{3}$$

where $x = 1 + y = 0{,}6 - 0{,}8$

Then:

$$P_z = C_p b S_z^x \sin^x \varphi \tag{4}$$

where b – cutting width, mm;

a – cut thickness, mm.

S_z – feed, mm/tooth.

φ – instant contact angle, °

The circumferential force has the maximum value at the moment the tooth is detached from the processed material:

$$P_{zmax} = C_p B S_z^x \sin^x \theta \tag{5}$$

where B – milling width, mm;

θ – milling cutter’s angle of contact with a workpiece, °.

If several teeth are in operation at the same time, for example 1 and 2, then cumulative circumferential force will be defined as:

$$P_{zcyм} = C_p b S_z^x (\sin^x \varphi_1 + \sin^x \varphi_2) \tag{6}$$

The given expression for $P_{zcyм}$ will also correspond to the maximum value of the circumferential cumulative force P_{zmax} because it corresponds to the moment of the next tooth is detached from the processed material [5,6]. The circumferential force creates a resistance moment against cutting and bends a mandrel:

$$M = \frac{P_z D}{2} \tag{7}$$

where M – torque, H-mm;

D– milling cutter diameter, mm.;

The maximum torque value will be:

$$M_{max} = \frac{P_{zmax} D}{2} = C_p B S_z^x \frac{D}{2} \sum_1^m \sin^x \varphi \tag{8}$$

To determine values of the feed force Ps and vertical force P when it comes to counter milling, we design all forces on horizontal X and vertical Y axes. Then the feed force will be:

$$P_s = P_{z1} \cos \varphi_1 + P_{z2} \cos \varphi_2 + P_{y1} \sin \varphi_1 + P_{y2} \sin \varphi_2 \tag{9}$$

The feed force will have the greatest value at the moment when the next tooth is detached from the processed material, then:

$$P_{zmax} = \sum_1^m P_z \cos\varphi + \sum_1^m P_y \sin\varphi \qquad (10)$$

It has been experimentally established that [2]:

$$P_y = (0{,}3; \dots; 0{,}35)P_z \qquad (11)$$

Assuming $P_y = 0.35P_z$, then:

$$P_{zmax} = C_p B S_z^x \left(\sum_1^m \sin^x\varphi \cos\varphi + 0.35 \sum_1^m \sin^{x+1}\varphi\right) \qquad (12)$$

Defining:

$$\sum_1^m \sin^x\varphi \cos\varphi = q; \qquad (13)$$

$$\sum_1^m \sin^{x+1}\varphi = q; \qquad (14)$$

Then:

$$P_{zmax} = C_p B S_z^x (q + 0.35p) \qquad (15)$$

We define vertical force P_v by using the following expression:

$$P_v = P_{z1}\cos\varphi_1 + P_{z2}\cos\varphi_2 + P_{y1}\sin\varphi_1 + P_{y2}\sin\varphi_2 \qquad (16)$$

Value P_v that corresponds the next tooth detachment from the processed material, will be defined as:

$$P_{v\varphi 2} = \sum_1^m P_z \sin\varphi + \sum_1^m P_y \cos\varphi \qquad (17)$$

When it comes to previously assumed values, we have:

$$P_{v\varphi 2} = C_p B S_z^x (q - 0.35p) \qquad (18)$$

The formula (18) for $P_{v\varphi 2}$ states that when p> 0.35 q the vertical force will tend to detach the part from the machine table, and when p <0.35 q it will press the part against the machine table. If we assume that one tooth is in contact with the part, then the part from the table is detached when p> 0.35 q, or:

$$\sum_1^m \sin^{x+1}\varphi > 0.35 \sum_1^m \sin^x\varphi \cos\varphi \qquad (19)$$

For the case of one tooth operation, we have:

$$\sin^{x+1}\varphi > 0.35\sin^x\varphi\cos\ \varphi \qquad (20)$$

$$\mathrm{tg}\ \ \varphi > 0.35 \qquad (21)$$

Using formula:

$$\theta > 115\sqrt{t/D} \qquad (22)$$

it is possible to determine at what ratio t/D a milling cutter will tend to detach the part:

$$115\sqrt{t/D}\ \ \geq \varphi \qquad (23)$$

The given ratio indicates that when applying a milling cutter with one tooth it will tend to detach the part from the table when $t/D \geq 0.03$.

Calculations show that if there are two teeth in operation at the same time, then the part detaches when $t/D \geq 0.045$.

According to [7,8], during the aging period when milling shaped surfaces of alloy steel, at the moment of contact of a processed part with blades of a milling cutter, forces arise with a maximum value of 1200N ÷ 1800N exceeding cutting forces in a stable mode 6 ÷ 8. As a result of aging of a milling cutter blade surfaces, cutting forces are reduced to stable values of 200N, because a tool has geometric parameters that are optimal for the given conditions. Graphs Series 1 ÷ 6 correspond to parameters of technological system accepted at an enterprise, and Series 7 ÷ 8 graphs correspond to optimized parameters which results in a significant reduction in cutting force.

Table 1 - Milling conditions

Parametrs	$\gamma,°$	$\alpha,°$	$\omega,°$	s, mm/tooth	t, mm	v, m/min
Series 1	5	20	15	0,20	2	18
Series 2	-5	20	15	0,20	2	18
Series 3	-5	30	15	0,20	2	18
Series 4	-5	30	10	0,20	2	18
Series 5	-5	30	10	0,08	2	18
Series 6	-5	30	10	0,08	1	18
Series 7	-5	30	10	0,08	1	13

The graph in Figure 1 shows that aging moment in the process of milling alloy steel is essential to establish reasons of wear proliferation and determine parameters of technological system. The less initial wear is a milling cutter blade has at the moment of aging, the slower the wear in the further stable mode.

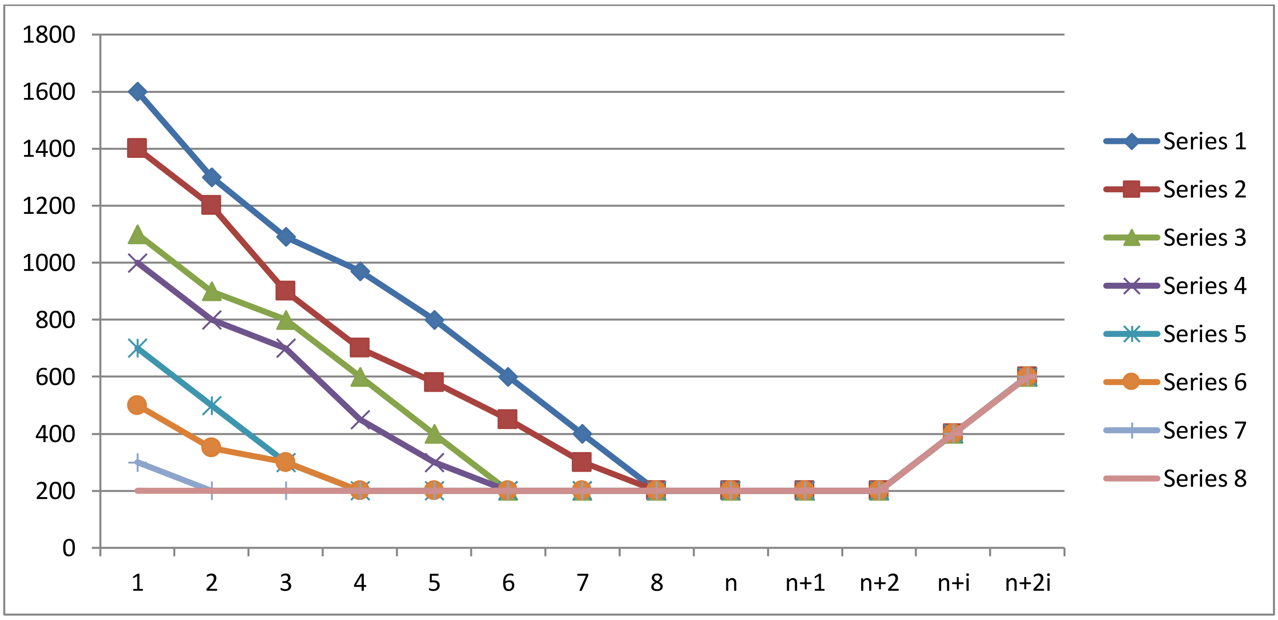

Fig.1. - Component force dependence P_z on the number of a milling cutter rotations

For machining shaped parts made of alloy steel, against a traditional tool, a milling cutter with a sharpened blade, shown in Figure 2, displayed durability. The negative front chamfer allows a milling cutter blade to withstand increased cutting forces which occur during aging when milling high-temperature alloys based on nickel avoiding negative consequences of the initial wear proliferation.

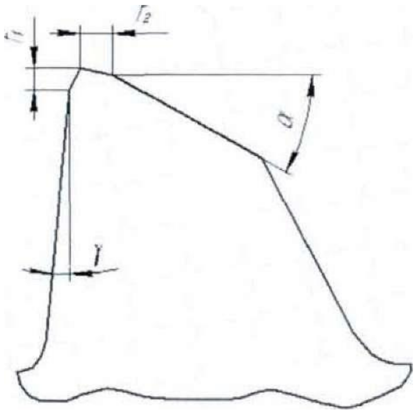

Fig.2. - Experimental form of sharpening of a milling cutter for machining alloy steel (geometric parameters: $\gamma = -5°$, $\alpha = 30°$, $\omega = 10°$)

According to [9,10], shapes of wear enable to make adjustments to geometric parameters of a milling cutter which in turn reduces aging time, and, hence, increases a tool life, thus, optimal geometric parameters of a milling cutter selected by visual analysis of a shape change of a blade during aging period.

3. Conclusion

Thus, by changing parameters of technological system, it is possible to change criterion of blade wear during aging period, and this, in turn, will increase a tool life, which will affect the increase in processing accuracy and increase productivity. Based on the results obtained and in accordance with the provisions of the theory of high-speed processing [4], it is most expedient to change the geometric parameters of the cutting tool.

4. References

[1] Neumoina N. G., Belov A. V. Thermal Processes in Technological Cutting System. - Volgograd: VolgGTU, 2006. - 84 p.
[2] Reznikov A.N., Reznikov L.A. Thermal Processes in Technological Systems. - M.: Mashinostroenie, 2007. 288 p.
[3] Reznikov A.N. Thermal Physics of Processes of Mechanical Processing of Materials. – M.: Mashinostroenie, 1981. - 279 p.
[4] Handbook of a Mechanical Engineer. In 2 volumes. Vol. 2 / ed. A.G. Kosilova, R.K. Meshcheryakova. M .: Mashinostroenie, 1986. - 496 p.
[5] Sherov K.T., Mardonov D.T., Buzauova T. M. The research of micro-hardness of side surface of teeth cylindrical wheels processed by 'shaved-rolling device' //Journal of Theoretical and Applied Mechanics, Sofia, Vol. 50, 2020. - P. 50-56
[6] Mashekov S.A., Smailova G.A., Kulgildinov M.S., Buzauova T. The study evolution of the structure formation of the foil workpiece during rolling screw rollers and longitudinal-wedge will (LWM) //Metalurgija 59, 3, 2020. - P.370-372.
[7] Yessirkepova A., Sherov K., Mikhailov V., Buzauova T. Research of ways of connecting reinforced bars in the production of reinforced concrete products //Journal of applied engineering science, 18(2020)3, 702. - P. 372 – 377.
[8] Auezova A., Abdugaliyeva G., Kurmangalieva L., Smagulova N., Buzauova T. Investigation of the stress-strain state of the roller conveyor //Metalurgija 59, 2, 2020. - P. 199 - 202
[9] Y. Adilkhanov, T.Buzauova, M. Murzakayeva. Experimental researching of dynamic quality and safety movement of half-wagons which have trolleys with diagonal connections. Journal of Engineering and Applied Sciences, 14 (16): 5831-5839, 2019, Pages 5831-5839.
[10] Alyzhanov M.K., Sikhimbayev M.R., Kuzembayev S.B., Sherov K.T., Buzauova T. M. Optimization of the conditions of convective drying of thermosensitive materials. //Journal of Theoretical and Applied Mechanics, Sofia, Vol. 46, No. 4, 2016. - P. 76-84

Information of the authors

Buzuova Toty Meyerbekovna, candidate of technical sciences, associate professor of the department "Technological equipment, mechanical engineering and standardization" of Karaganda Technical University
E-mail: toty_77@mail.ru

Smagulov Altai Serikovich, undergraduate of the department "Technological equipment, mechanical engineering and standardization" of Karaganda Technical University
E-mail: smagulovaltay@gmail.com

DOI 10.52209/2706-977X_2021_1_24 **IRSTI 55.51.09** **UDC 622.2:004.9**

Developing Design Documentation and Producing Technological Supporting Tools for Contour Rock Massif

Demin V.F., Kamarov R.K.*
Karaganda Technical University, Karaganda, Kazakhstan
***corresponding author**

Abstract. Scientific-design and applied studies for developing the design documentation and manufacturing technological tools for supporting the contour rock massif have been carried out. The terms of reference for developing the design documentation and producing a mine rope anchor with devices for assembling the rope anchor have been developed. A batch of prototypes of multipurpose laying systems for supporting mine workings has been manufactured at the Karaganda Machine-Building Consortium LLP with establishing the load parameters of rope anchors for maximum load and deformation. Technological designs of rope anchors have been successfully tested in the mines of the Karaganda coal basin.

Keywords: terms of reference, supporting, rock massif, rope anchor, parameter, load, deformation.

1. Introduction

The terms of reference provides for developing the design documentation and manufacturing an anchor that consists of several steel spring wires twisted into one strand and developing the manufacturing technology with the use of the existing equipment [1 - 8].

For manufacturing rope anchors, the following machines has been used: the K163screw-cutting lathe for turning work; the M135 drilling machine for drilling holes in workpieces; the 25-60 t press for swaging, pressing, fixing the rope parts; the welding machine; the spring-wound, for leveling spring wire, wire cutting; the Crystal 2 thermal cutting machine for plasma or arc cutting the supporting plate; the vertical milling machine for manufacturing keyways, keys, milling parts.

To carry out this work, a working group has been formed that consists of 7 people: a design engineer, a technologist, a shop mechanic, 2 repairmen, a turner and a milling machine operator.

In the process of design documentation (CD), the selection of materials, the development and approval of the technical proposal, the manufacture and testing of material models (experimental samples), the manufacture and preliminary testing of the prototype and the correction of the CD based on the results of the prototype were made.

Below there is a description of the process stages of manufacturing a mine rope anchor.

The twisting of the wires has been carried out using a lathe with previously clamped wires in the lathe chuck (see Figure 1). A spring wire with the diameter of 3 - 5 mm and the length of 2.0 - 2.5 m has been used so that one could observe how the wire would behave.

Due to the fact that the lathe chuck has 3 jaws, the clamping of the sleeve was performed unevenly. When twisting, the wire slipped, it did not twist into a common strand and the appearance of the anchor did not correspond to the generally accepted standard, there was no uniform tension and therefore, such an anchor would not technologically perform its main function, carry vertical and tangential loads, torque in this case would work with the smallest loads.

The laboratory testing of the spring wire for breaking has confirmed its technical characteristic that makes 1830 N/mm^2. To increase the breaking capacity, only spring wire with the diameter of 6 mm has been used in the rope anchors. The clamping sleeve has been cut into 3 parts, like the clamps on a lathe, however, laying the wire, holding it, inserting it into the lathe chuck has caused a lot of inconvenience.

For quick mounting and convenience, a sleeve has been used that consists of 3 parts, to fix it with a ring. To improve safety and the assembling technology, a second lathe has been used. It has been located at the distance of 5.5 m from the first one. Such a scheme made it possible to produce anchors of a certain length and perform uniform twisting of the wire. In the first lathe, the anchor has been fixed, and on the second one the minimum rotation for twisting the wires has been developed, i.e. 16 rpm.

In the work, lathes of the 1K62 brand have been used. The scheme of their location is shown in Figure 1, f.

In the process of finalizing the technology according to this technique, a number of comments and additions have been identified: spring wire that is in the coil after cutting 5.5 m in length is twisted in a spiral, in this regard, additional work has been required to level it manually. This work has been carried out by two workers to ensure that the wire does not slip and twists evenly.

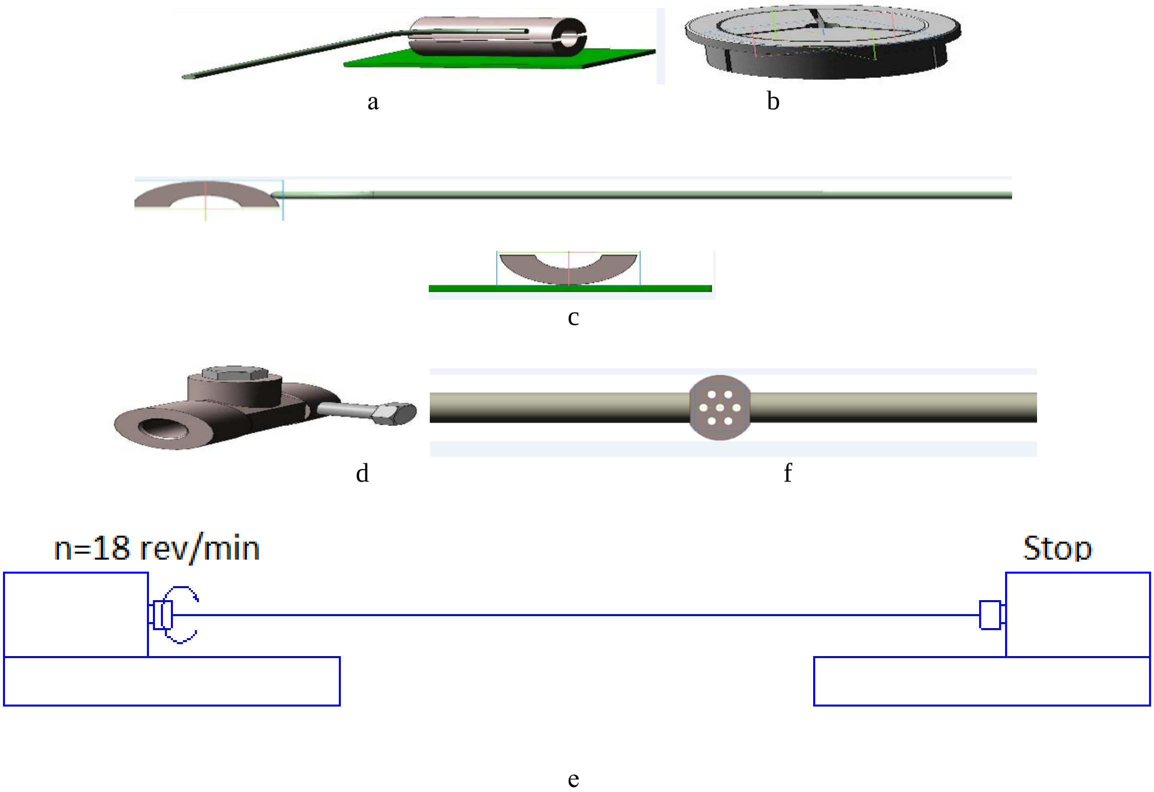

Fig. 1. – Facilities for the rope anchor assembling

To produce mine anchors on a production scale, the work has been improved to flatten the wire and reduce the number of workers. For this purpose, additional equipment has been designed and manufactured.

A batch of anchors of various lengths from 2.0 to 5.5 m with the use of various spring wire diameters from 4 to 6 mm has been produced.

The use of the A5218 spring-coiling machine has made it possible to untwist and straighten the wire of the same length and to produce its automatic cutting; the fastening nut and the tapered fastening sleeve have been manufactured on the 1K62 lathe; the thrust washer has been manufactured using a gas-cutting unit (plasmatron); the design of the clamping sleeve has been changed. It is a T-shaped blank with a hole inside for placing a spring wire and two bolts for fixing a T-shaped clamping sleeve, which prevents it from turning in the chuck of the lathe. The bolt used to fix the wires in the mandrel is made with a ball with the diameter of 9 mm rolled at the end. This allows fastening the wires securely and in the future unscrewing and removing easily the mandrel from the wire. Figure 1, d shows the used clamping sleeve (mandrel with a bolt). For preliminary uniform twisting of the spring wire, a device has been used that consists of a flat sleeve of the body with 7 holes (according to the number of wires in the strand); handles for manual scrolling of the wire have been welded on the sides.

The following is a description of the process of assembling the rope anchor using the developed technology. From a coil mounted on a support, the wire is passed through a spring-coiling machine (A 5218 model), where the wire is leveled and cut with a special device in the size of 5.5 m in the amount of 7 pieces for 1 anchor.

Then, the wire has been transferred to the section of the anchor assembly, where it has been alternately passed through a pipe with the diameter of 20 mm and the length of 1 meter, then there has been inserted a washer with the diameter of 200 mm and the thickness of 6-10 mm with an inner hole with the diameter of 16 mm, then a threaded conical bushing-cone has been mounted (Figure 1 d), onto which a 55 mm hex nut with M36 thread has been screwed.

At the end of the entire assembled structure, a T-shaped clamping sleeve has been mounted and the wires have been clamped in two planes using bolts. Then the clamping sleeve has been placed in the chuck of the lathe and fixed. The device has been placed on the free end of the anchor, the mandrel, where each wire has been passed through the hole and all these have been dragged along the wire to the beginning of the anchor.

In this state, holding the mandrel handle, several rotations have been performed with gradual movement to the free end of the anchor; from spontaneous unwinding of wires with the diameter of 6 mm, the bundle has been fixed with temporary clamps. A binding wire set at a certain distance has been used as temporary clamps.

After twisting the anchor wires manually, the mandrel fixture has been removed, and a fastening sleeve has been mounted for further crimping of the anchor end. The fixing sleeve has the following characteristics for a wire with the diameter of 6 mm: the length is 30 mm; the inner size is 19 mm; the outer size is 27 mm.

A second fixing sleeve has been mounted, and the position of the wires has been fixed with bolts; the entire structure has been clamped in the chuck of the second lathe, after which mechanical make-up began at minimum speed (16 rpm) with obtaining a uniform tight lay along the entire length of the anchor. The rotation has been stopped, and the entire system has been left at rest for 10 - 15 minutes. After that, the anchor is removed from the lathe chucks and transferred to the assembly area, where the clamping sleeves are removed from both ends.

From the side of the tapered sleeve, the wires have been wedged, for this a wedge has been driven into the tapered sleeve and the excess ends of the wire have been cut off with a grinder. A press has been used to crimp the mounting sleeve located at the second end of the anchor. Using a device for crimping the mounting sleeve, it has been fixed.

A matrix and a punch have been used as a device (Figure 1, c). The press pressure is 630 kg/cm^2. With the help of the grinder, the excess ends of the wire have been cut off. The anchor is rigidly connected to each other by all the parts; the clamping sleeve has an outer diameter of 26 mm, because borehole diameter is 228 mm; the stiffening tube has the outer diameter of 26 mm and the length of 1200 mm; the inlet hole on the base plate has the diameter equal to the outer diameter of the stiffening tube; the threaded connection for the anchor nut is located on the stiffening tube, which in turn has been rigidly connected to the rope at the outlet; the threaded connection has the diameter for the standard M24 nut and the thread length of at least 250 mm for mounting the anchor using the Super Turbo Bolter plant with a standard adapter.

The design correction of the support sleeve has been substantiated: the thread length is 250 mm with the M-36 nut, since it is technologically impossible to execute the M-24 nut: when the diameter of the sleeve decreases, it loosens and deforms when the nut is tightened (Fig.2).

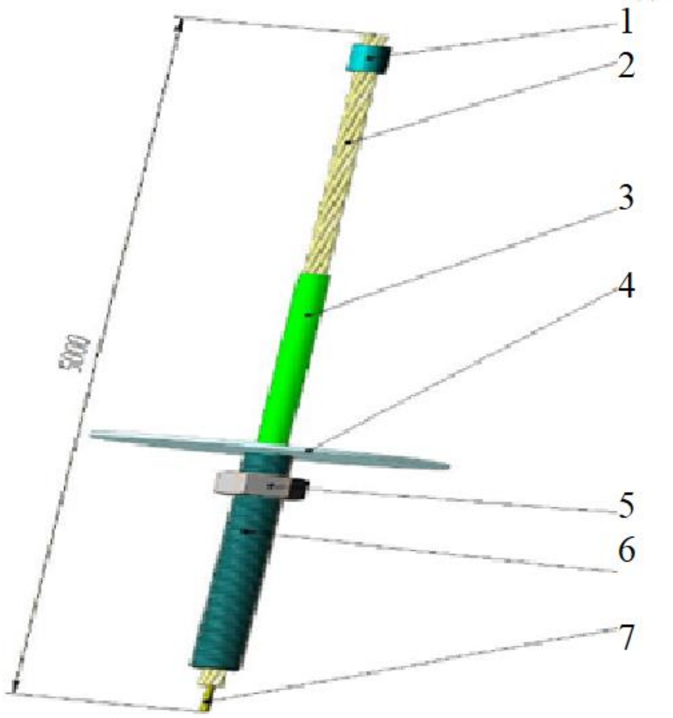

1 - clamping sleeve; 2 - rope of 7 steel wires; 3 - stiffening pipe; 4 - supporting plate; 5 - anchor nut; 6 – cone; 7 - metal wedge

Fig.2. – The АКМК 1 anchor design

The anchor is made of several steel wires twisted into one braid with the length of 5.5 m.

The material characteristics are as follows: steel yield strength within 570 - 620 N/mm^2; tensile strength must be at least 20 % higher than yield strength; when checked for tension, the anchor must not fail at the load that is lower than 295 kN.

The base plate should be made of rolled steel 6 mm thick, 200 × 200 mm in size with a central hole.

The anchor must have a stiffening pipe, with the help of which the anchor is mounted. The stiffening pipe has side slots that allow entering the polymer composition inside the tube; the dimensions of the stiffening tube are as follows: L = 1200 mm, the outer diameter is 25 mm, the inner diameter is 20 mm.

2. Results and discussion

Based on the results of laboratory studies, it has been proposed to make the anchor braid using the B-2-6 wire, GOST 9389-75, steel 60S2 with the diameter of 6 mm, the yield point $[\delta_т]$ = 1570 N/mm^2; tensile strength $[\delta\ \delta_{вр}]$ = 1770 N/mm^2; the number of wires in the anchor braid is 7.

The calculation of the load-bearing capacity of the anchor has been performed with determining the anchor cross-section:

$$S_{chek} = 28{,}26\ mm^2,\ S_{com} = S_{chek}\times 7 = 197.82\ mm^2.$$

According to this data, the anchor braid will have the following bearing capacity:

$$N = [\delta_{rot}] \times S_{com} = 1770\times 197.82 = 350141\ H = 350.141kN.$$

This material meets the parameters of the technical specifications.

When developing the design documentation, three options for the anchor layout have been proposed:

- fastening the anchor braid in the body using a wedge (Fig. 3);

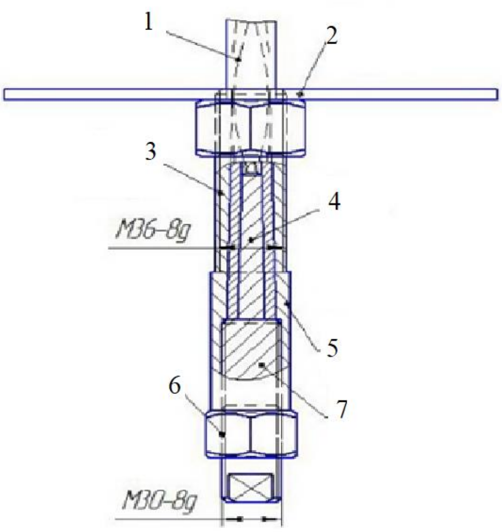

1 - stiffening pipe; 2 - supporting plate; 3 - anchor braid; 4 – wedge; 5 - anchor body; 6 - nut M30, 7 - pin

Fig. 3. – Fastening the anchor braid in the body using a wedge

- fastening the anchor braid using a wedge, a pin and filling the voids in the anchor body with lead (Fig.4);

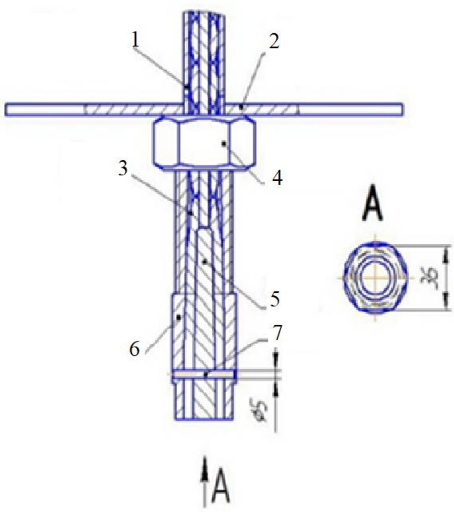

1 - stiffening pipe, 2 - supporting plate, 3 - anchor braid, 4 - nut M36, 5 - wedge, 6 - anchor body, 7 - pin

Fig. 4. – Fastening the anchor braid using a wedge, a pin and filling the voids in the anchor body with lead

- fastening the anchor braid using a ball wedge (Fig. 5).

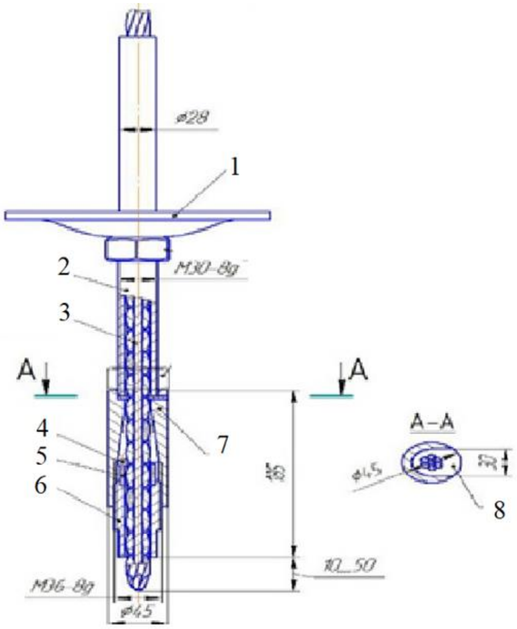

1 - key-damping plate; 2 - clamping sleeve; 3 - anchor braid; 4 – ball; 5 – cone; 6 - anchor nut; 7 – body; 8 - supporting plate

Fig. 5. – The design correction

When testing the anchor in industrial conditions with the anchor braid attached to the body (Fig. 3), a significant drawback has been revealed: when the anchor was loaded, the anchor wires were deformed and, as a consequence, the anchor braid simply slipped out of the body over time, which led to the destruction of the anchor attachment.

Therefore, another layout decision has been made: fastening the anchor braid using a wedge, a pin and filling the voids in the anchor body with lead (Fig. 4). The pin does not allow moving the wedge, and the lead the possibility of the wires of the anchor braid deformation, while eliminating the possibility of the anchor braid slipping out of the anchor piece. This fastening of the anchor braid has a disadvantage: complexity of manufacturing.

In addition to fastening the anchor braid to the body using a smooth wedge, it is proposed to perform this fastening using a ball wedge. The function of a wedge is performed by balls that are located in the grooves between the strands of wires and expand against the surface of the body inclined to the cylindrical hole by rolling when the anchor braid is pulled out during the pre-tensioning process. The inclined surface of the body brings the balls closer together, which compress the braid of the anchor. Then, the anchor braid does not have the ability to move relative to the body in the axial direction due to the fact that the rolls cannot slip the balls, because they cannot reduce their volume. In order for the anchor braid to slide over the balls, it needs rotation around the axis. It does not have this opportunity due to friction against the walls of the body and due to the fact that the washer is mounted at the inlet of the body made with a hole that repeats the profile of the anchor braid (Fig.5). This anchor fastening seems to be more reliable than the previous ones, and from the point of view of manufacturing it is more technologically advanced.

A pilot batch of rope anchors with progressive innovations implemented in the submitted patent applications for inventions [9 - 10] has been manufactured at the Karaganda Machine-Building Consortium LLP.

The manufacturing technology of rope-cable supporting tools includes the following technological processes: straightening the spring wire from circular coils; producing tension nuts, a fixing sleeve, base plates (Fig.6); mounting a support plate, the fixing sleeve and its wedging; twisting the wire rods (Fig. 7); pressing the annular end piece onto the end (Fig. 8); placing the fixing wires along the fastening tool.

The laboratory tests of the spring wire for rupture have confirmed its technical characteristic that makes 1830 N/mm^2. To increase the breaking characteristic, it is proposed to use a spring wire with the diameter of 6 mm in the supporting tools.

Fig. 6. – Manufacturing and mounting the support plate, the fixing sleeve and its wedging

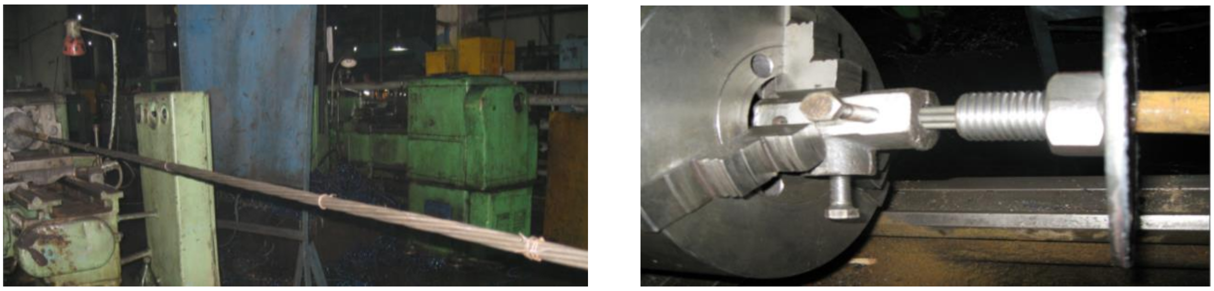

a) b)

a) general view of the lathe; b) wire in the chuck

Fig.7. – Twisting the wire rods on the adjacent-spaced machines

a) b)

a) assembly type; b) the wire in the clip

Fig. 8. – Pressing the end ring on the anchor

This material satisfies the parameters of the technical specifications. The layout of the rope anchor design is shown in Fig. 9.

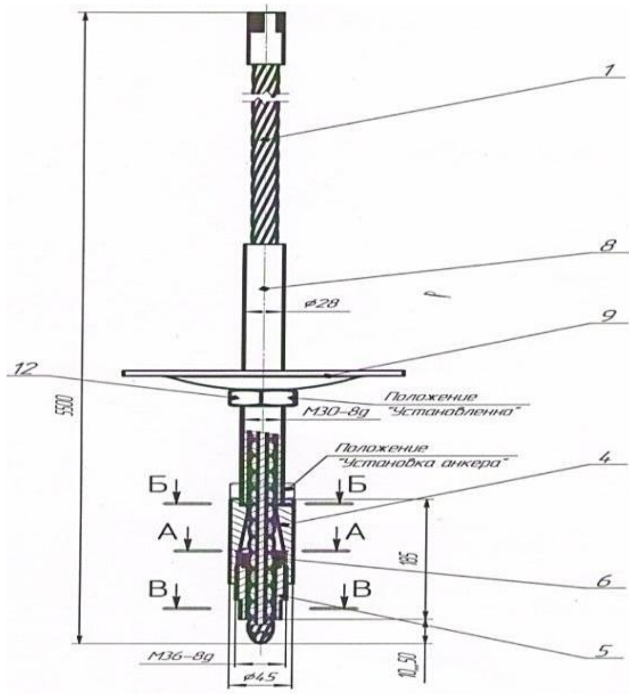

1 - rope; 4 - clip; 5 - pins; 6 - saddle; 8 - guide tube; 9 - base plate; 12 - clamping nut

a)

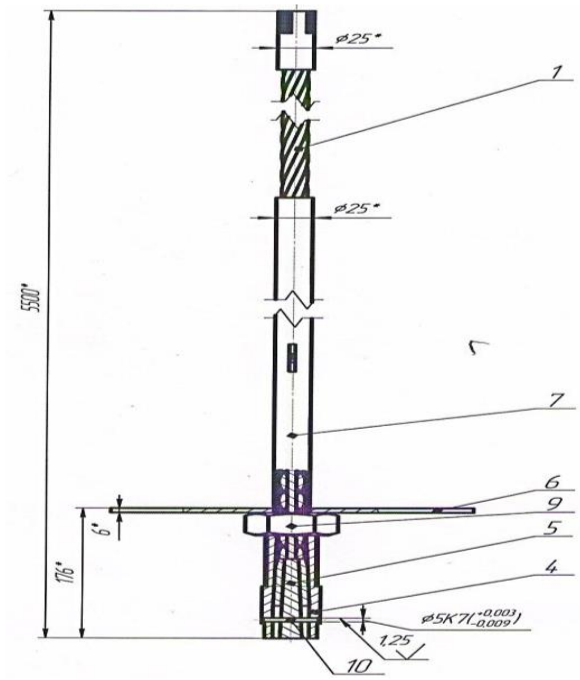

1 - rope; 4 - clip; 5 - pin; 6 - base plate; 7 - guide tube; 9 - clamping nut

b)

c)

d)

a, c - a spacer and a slot in the cone clip and a sleeve; b, d - petal-collet and sleeve

Fig. 9. – Layout of the rope anchor with a wedge clamping connection in the supporting sleeve, sheet 1

e

f

g

e) manufacturing supporting sleeves; f) studies to determine methods of wire fixing in the supporting sleeve; g) pressing the edge

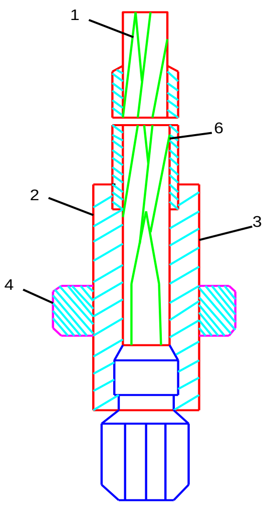

e)

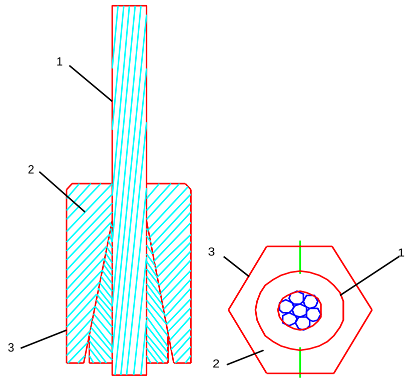

f)

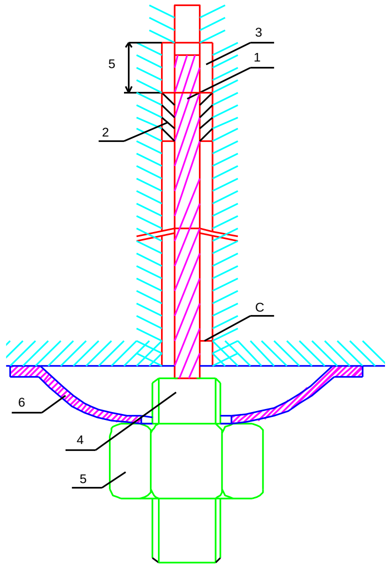

g)

1 – rope; 2, 3 – supporting sleeve clip и and sleeve itself; 4 – supporting plate

1 – rope; 2, 3 – wedged supporting sleeve and its clip

1 – rope; 2 – centering rings; 3 – the hole (well) cavity; 4 – supporting sleeve; 5 – retaining nut; 6 – supporting plate

Fig. 9. – Layout of the rope anchor with a wedge clamping connection in the supporting sleeve, sheet 2

Figure 10 shows the layout of the rope anchor with a wedge clamping connection in the supporting sleeve.

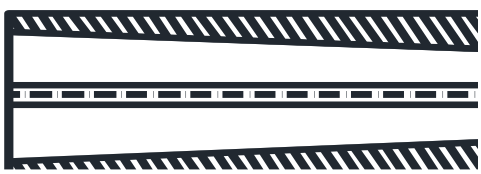

h)

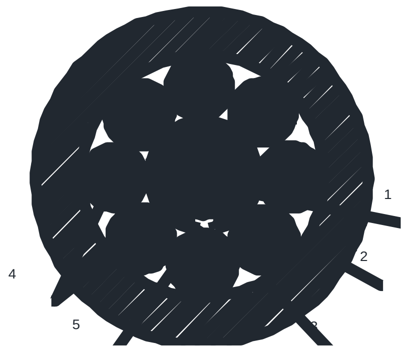

i)

h, i - supporting sleeve profile and its section
1 - central wedge; 2, 3 - outer and inner surfaces of the sleeve clip; 4 - strands of rope; 5 - clamping centering ring

Fig. 10. - The layout of the rope anchor with a wedge clamping connection in the supporting sleeve, sheet 3

Figure 11 shows the prototypes of rope anchors manufactured at the Karaganda Machine-Building Consortium

LLP.


a)


b)


c)


d)

a, b - views from the end and side, respectively; b, d - end and mouth parts

Fig. 11. - Prototypes of rope anchors manufactured at the Karaganda Machine-Building Consortium LLP

Figure 12 shows testing the rope anchor structures on the test bench of the Karaganda Promstroyproekt Institute LLP.

The laboratory testing of the spring wire for rupture has confirmed its technical characteristic that makes 1.83 kN/mm^2. To increase the breaking capacity, it has been proposed to use only 6 mm diameter spring wire in anchors.


a)


b)

a) general view of the bench; b) testing the wire for breaking

Fig.12. – Testing rope anchor designs (Promstroyproyekt LLP)

Bench testing the rope and cable anchors have been carried out at the test site of the KLMZ plant of the Kazakhmys Corporation LLP (Fig.13).


a)


b)


c)

a, b) prepared for breaking respectively rope and cable anchors; c) broken rope anchor

Fig. 13. – Bench testing the rope anchors, sheet 1

d) e) f)

d) broken cable anchor sleeve; d) test bench; e) computer for taking load characteristics

Fig. 14. - Bench testing the rope anchors, sheet 2

Figure 15, in accordance with the presented test reports, establishes the load parameters of the rope anchors for the maximum load (kN) and deformations (mm).

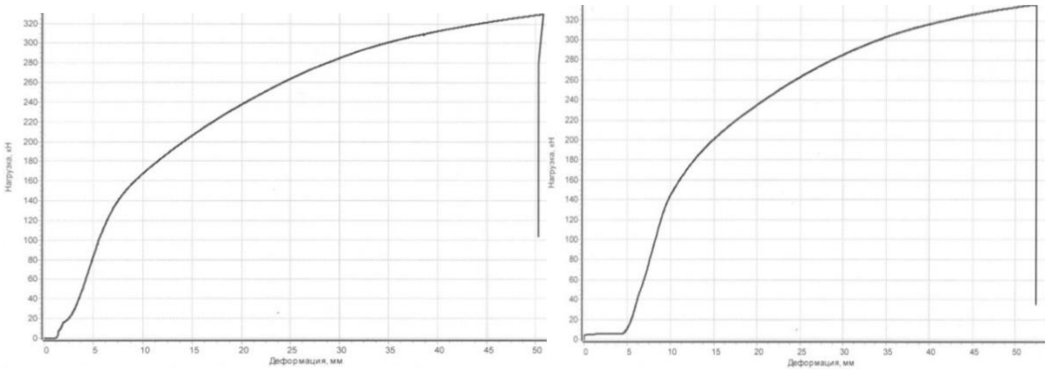

a) b)

Fig. 15. - Load parameters when testing rope anchors (a, b respectively): maximum load 351, 346 - 330 kN; maximum deformations 55.9; 48 - 34.3 mm

3.Conclusion

Scientific-design and applied studies for developing the design documentation and manufacturing technological tools for supporting contour rock massif have been carried out.

The terms of reference for developing the design documentation and manufacturing a mine rope anchor with devices for assembling a rope anchor have been developed. The design correction of the suppoing sleeve has been substantiated: the thread length is 250 mm with the M-36 nut, since it is technologically impossible to execute the M-24 nut: when the diameter of the sleeve decreases, it loosens and deforms when the nut is tightened.

When developing the design documentation, three options of the anchor layout have been proposed: fastening the anchor braid in the body using a wedge; fastening the anchor braid using a wedge, a pin and filling the voids in the anchor body with lead; fastening the anchor braid with a ball wedge. The balls are located in the grooves between the wire strands and expand against the body surface inclined to the cylindrical hole by rolling when the anchor braid is pulled out during the pre-tensioning process. This anchor fastening seems to be more reliable than the previous ones, and from the point of view of manufacturing it is more technologically advanced.

A batch of prototypes of multipurpose laying systems for supporting mine workings has been manufactured at the Karaganda Machine-Building Consortium LLP. The batch of rope anchors has been made with progressive innovations implemented in patents for inventions.

The manufacturing technology of rope-cable supporting tools includes the following technological processes: straightening the spring wire from circular coils; producing tension nuts, fixing couplings, base plates; mounting a support plate, fixing a sleeve and its wedging; twisting wire rods; pressing the end ring onto the end; mounting fixing wires along the length of the supporting tools.

The laboratory testing of the spring wire for breaking have confirmed its technical characteristic that makes 1830 N/mm^2. To increase the breaking characteristic, it is proposed to use a spring wire with the diameter of 6 mm in the supporting tools.

Bench testing the rope anchor structures have been performed at the test bench of the Karaganda Promstroyproekt Institute LLP and at the test ground of the KLMZ plant of the Kazakhmys Corporation LLP with establishing the load parameters of the rope anchors for maximum load and deformations. The substantiated load parameters during testing the rope anchors have been as follows: the maximum load is 351, 346, 330 kN; deformation is 55.9; 48; 340.3 mm.

The technological designs of the developed rope anchors have been successfully tested in the mines of the Karaganda coal basin.

4. References

[1] Pivnyak G., Bondarenko V. Kovalevska I. Mining of Mineral Deposits. A Balkema Book. CRC Press is an imprint of the Taylor & Francis Group an informa business. London. 2014. – 371 p.
[2] Kowaltchuk A.B. NeuesKonzeptdei der Projektierung und Herstellung der Strebausrüngungen. «Gluckauf», 3, Maj, No. 1 (2), 2003. - P. 20 - 23.
[3] Tsai B.N. Thermally activated nature of rock strength. Karaganda: KSTU, 2007. - 204 p.
[4] Osipov A.N., Bulkin A.V., Guselnikov L.M., et al. Method of fighting against heaving of the mine workings soil (RF patent No. 2438018). Published on 12/27/2011.
[5] Zatsepin A.S., Pleskunov I.V. Method of protecting local development workings (RF patent No. 2338066). 12/27/2011.
[6] Rozenbaum M. A., Demekhin, D. N. Deformational criteria for the stability of roof rocks and rock bolts. Journal of mining science. Volume: 50, Issue: 2, 2014. - Pages: 260264. DOI: 10.1134 / S1062739114020082.
[7] Nierobisz A. Development of roof bolting use in Polish coal mines. Journal of mining science. Volume: 47 Issue: 6 Pages: 751760. Published: Nov. 2011. View Journal Information.
[8] Borsch-Komponiyets V.I. Practical rock mechanics. A guide-book for mining engineers. M.: Publishing house "Gornaya kniga", 2013. - 322 p.
[9] Demin V.F., Issabek T.K., Mussin R.A., et al. Method of fastening the working roof. Patent No. 34092. publ. 12/27/2019. Bul. No. 52. - 3 p.
[10] Demin V.F., Issabek T.K., Mussin R.A., et al. Method of supporting mine workings. Patent No. 33721. publ. 06/28/2020. Bul. No. 26. - 3 p.

Information of the authors

Demin Vladimir Fedorovich, doctor of technical sciences, professor of the department "Development of mineral deposits" of Karaganda Technical University
E-mail: vladfdemin@mail.ru

Kamarov Rymgali Kumashevich, doctor of technical sciences, professor of the department "Development of mineral deposits" of Karaganda Technical University
E-mail: ipk@kstu.kz.